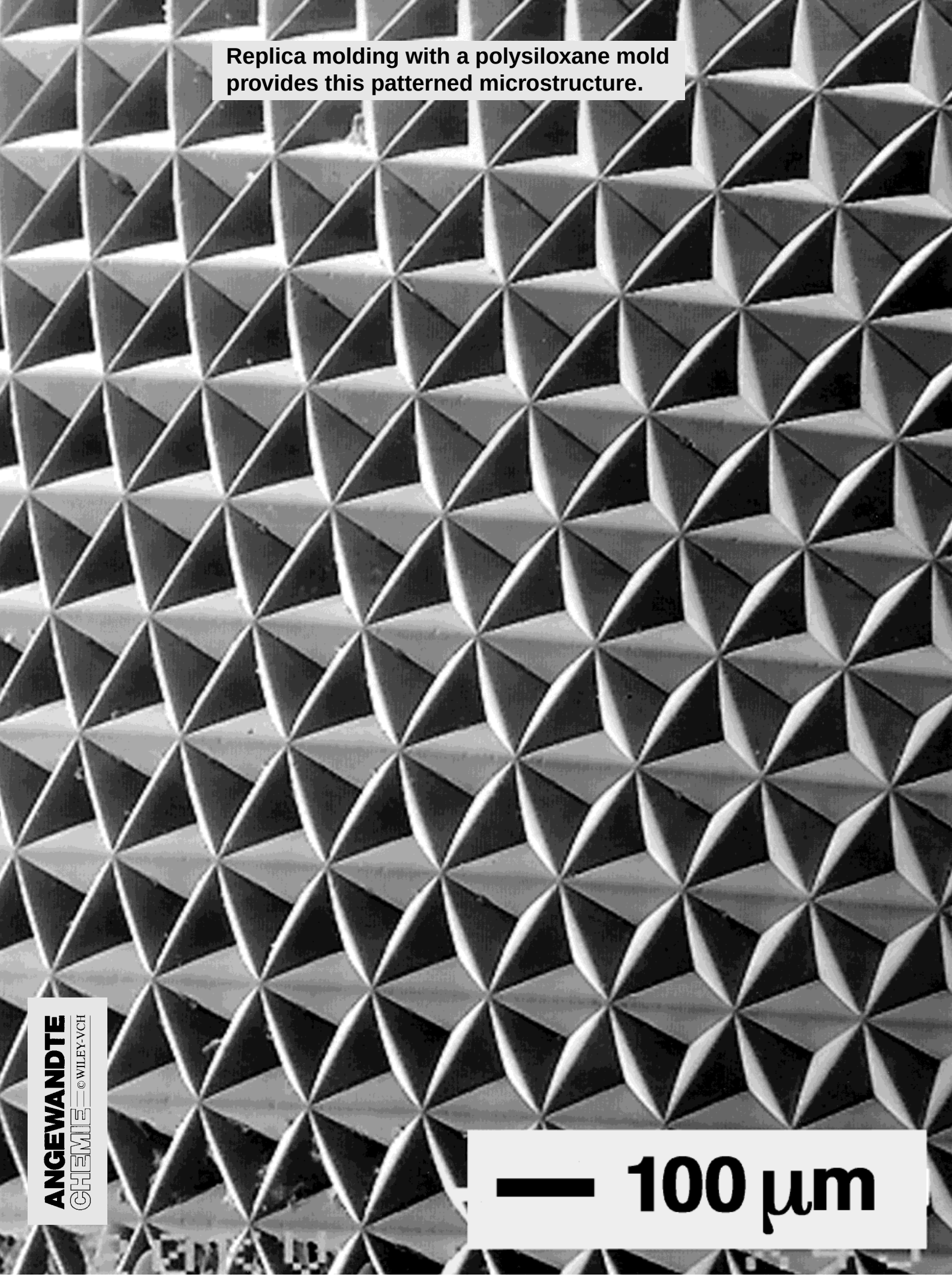

Soft Lithography

Younan Xia and George M. Whitesides*

Microfabrication, the generation of small structures, is essential to much of modern science and technology; it supports information technology and permeates society through its role in microelectronics and optoelectronics. The patterning required in microfabrication is usually carried out with photolithography. Although it is difficult to find another technology with more dominant influence, photolithography nonetheless has disadvantages. The sizes of the features it can produce are limited by optical diffraction, and the high-energy radiation needed for small features requires complex facilities and technologies. Photolithography is expensive; it cannot be easily applied to nonplanar surfaces; it tolerates little variation in the materials that can be used; and it provides almost no control over the chemistry of patterned surfaces, especially when complex organic functional groups of the sorts needed in chemistry, biochemistry, and biology are involved. We wished to develop alternative, non-photolithographic microfabrication methods that would complement photolithography. These techniques would ideally circumvent the diffraction limits of photolithography, provide access to three-dimensional structures, tolerate a wide range of materials and surface chemistries, and be inexpensive, experimentally convenient, and accessible to molecular scientists. We have developed a set of such methods that we call "soft lithography", since all members share the common feature that they use a patterned elastomer as the mask, stamp, or mold. We describe here soft lithography, and survey its ability to provide routes to high-quality patterns and structures with lateral dimensions of about 30 nm to 500 μm in systems presenting problems in topology, materials, or molecular-level definition that cannot (or at least not easily) be solved by photolithography.

Keywords: elastomers · materials science · patterning · supramolecular chemistry

1. Introduction

The ability to generate small structures is central to modern science and technology. There are many opportunities that might be realized by making new types of small structures, or by downsizing existing structures.[1] The most obvious examples are in microelectronics, where "smaller" has meant better—less expensive, more components per chip, faster operation, higher performance, and lower power consumption—since the invention of transistors in 1947.[2] It is also clear that many interesting new phenomena occur at nanometer dimensions: Examples include electronic processes such as quantum size effect (QSE),[3] Coulomb blockade,[4] and single-electron tunneling (SET).[4]

Microfabrication has its foundations in microelectronics, and it will continue to be the basis for microprocessors, memories, and other microelectronic devices for information technology in the foreseeable future. It is also increasingly being applied in areas outside of microelectronics (Figure 1).[5–9] Miniaturization and integration of a range of devices have resulted in portability; reductions in time, cost, reagents, sample size, and power consumption; improvements in detection limits; and new types of functions.

Photolithography is the most successful technology in microfabrication.[10] It has been the workhorse of semiconductor industry since its invention in 1959: Essentially all integrated circuits are made by this technology. The photolithographic techniques currently used for manufacturing microelectronic structures are based on a projection-printing system (usually called a stepper) in which the image of a reticle is reduced and projected onto a thin film of photoresist that is spin-coated on a wafer through a high numerical aperture lens system. The resolution R of the stepper is subject to the limitations set by optical diffraction according to the Rayleigh Equation (1),[10a] where λ is the wavelength of

$$R = k_1\lambda/\mathrm{NA} \quad (1)$$

the illuminating light, NA the numerical aperture of the lens system, and k_1 a constant that depends on the photoresist. Although the theoretical limit set by optical diffraction is usually about $\lambda/2$, the minimum feature size that can be ob-

[*] Prof. G. M. Whitesides, Dr. Y. Xia
Department of Chemistry and Chemical Biology
Harvard University
12 Oxford Street, Cambridge, MA 02138 (USA)
Fax: (+1) 617-495-9857
E-mail: gwhitesides@gmwgroup.harvard.edu

  1433-7851/98/3705-0551 $ 17.50+.50/0

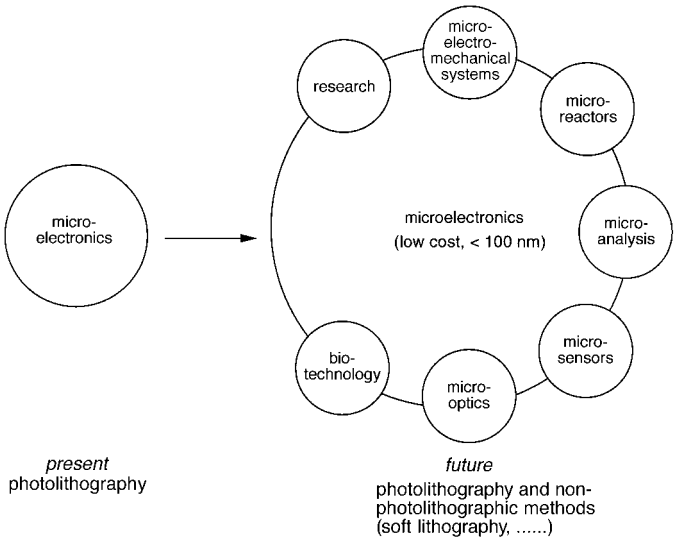

Figure 1. Microelectronics is based on photolithography and is very important, but the more expensive technology to surmount the "100-nm barrier"—a critical point in reducing feature sizes set by a combination of diffraction limitations to projected images and the lack of lenses that are transparent at wavelengths below 160 nm—make the future of photolithography on this small scale unclear. In addition, new opportunities in microfabrication are emerging as new types of microsystems (right) are developed; for these opportunities, photolithography is not always the best option. For most applications, cost is a dominant parameter.

tained is approximately the wavelength (λ) of the light used. As a result, illuminating sources with shorter wavelengths are progressively introduced into photolithography to generate structures with smaller feature sizes (Table 1).[10c] As structures become increasingly small, they also become increasingly difficult and expensive to produce.

In the late 1960s and early 1970s, Gorden Moore, founder of both Fairchild Semiconductor and Intel, projected that the number of transistors in an integrated circuit would double every 18 months or so. This prediction was later known as Moore's Law.[2] Over the past three decades many trends in the semiconductor industry have followed this law (Figure 2) thanks to continuous developments in photolithography that have allowed the size of features to decrease by a factor of approximately one-half every three years (Table 1). It is plausible that features as small as 100 nm can be manufactured optically in the future by employing advanced mask/resist technologies and deep UV (DUV) radiation.[10d] Below this size, however, it is generally accepted that current strategies for photolithography may be blocked by optical diffraction and by the opacity of the materials used for making lenses or supports of photomasks. New approaches must be developed if Moore's Law is to extend into the range below

Table 1. The recent past, present, and future of semiconductor technology.[10c, 12]

Year	Lithographic method	Resolution [nm][a]	Bits (DRAM)[b]
	Photolithography (λ[nm])		
1992	UV (436), *g* line of Hg lamp	500	16 M
1995	UV (365), *i* line of Hg lamp	350	64 M
1998	DUV (248), KrF excimer laser	250	256 M
2001	DUV (193), ArF excimer laser	180	1 G
2004	DUV (157), F_2 excimer laser	120	4 G
2007	DUV (126), dimer discharge from an argon laser	100	16 G
2010	*Advanced lithography*	<100[c]	>16 G
	extreme UV (EUV, 13 nm)		
	soft X-ray (6–40 nm)		
	focused ion beam (FIB)		
	electron-beam writing		
	proximal-probe methods		

[a] The size of the smallest feature that can be manufactured. [b] The size of the dynamic random access memory (DRAM). [c] These techniques are still in early stages of development, and the smallest features that they can produce economically have not yet been defined.

Younan Xia was born in Jiangsu, China, in 1965. He received a B.S. degree from the University of Science and Technology of China in 1987, and then worked as a graduate student for four years at the Fujian Institute of Research on the Structure of Matter, Academia Sinica. He came to the United States in 1991, and received a M.S. degree from the University of Pennsylvania (with A. G. MacDiarmid) in 1993 and a Ph.D. degree from Harvard University (with G. M. Whitesides) in 1996. He is currently Assistant Professor of Chemistry at the University of Washington in Seattle. His research interests include micro- and nanofabrication, self-assembled monolayers, inorganic functional materials, nanomaterials, conducting polymers, microanalytical systems, microelectromechanical systems, and novel devices for optics, optoelectronics, and display.

Y. Xia

G. M. Whitesides

George M. Whitesides was born in 1939 in Louisville, Kentucky, USA. He received an A.B. degree from Harvard University in 1960 and a Ph.D. degree from the California Institute of Technology (with J. D. Roberts) in 1964. He was a member of the faculty of the Massachusetts Institute of Technology from 1963 to 1982. He joined the Department of Chemistry of Harvard University in 1982 and was department chairman from 1986 to 1989; he is now Mallinckrodt Professor of Chemistry. His present research interests include biochemistry, surface chemistry, materials science, molecular virology, optics, self-assembly, bioanalytical chemistry, microelectromechanical systems, and microfluidics.

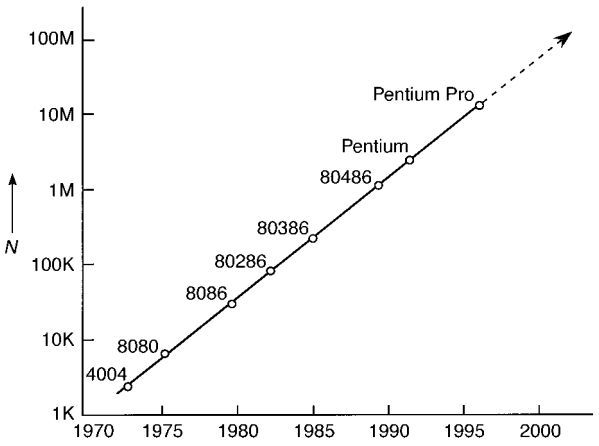

Figure 2. The integration trend given by Moore's law, and how microprocessors manufactured by Intel have followed this law since 1973;[2b, c] N = number of transistors per chip. This curve reflects the general trend of miniaturization achieved by microlithography; it also applies to other devices such as RAMs, DRAMs, and Motorola microprocessors.

100 nm. Advanced lithographic techniques currently being explored for this regime include extreme UV (EUV) lithography, soft X-ray lithography, electron-beam writing, focused ion beam writing, and proximal-probe lithography.[11, 12] These techniques are capable of generating very small features, but their development into practical commercial methods for low-cost, high-volume processing still requires great ingenuity: EUV and X-ray techniques, for example, will probably require the development of reflective optics.[10d]

The continued shrinking of feature sizes toward 100 nm poses new technical challenges for photolithography, but, even for microfabrication on the micrometer scale, it may not be the only and/or best microfabrication method for all tasks. For example, it is expensive (both in capital and operating cost), which makes it less than accessible to chemists, biologists, and material scientists; it cannot be easily adopted for patterning nonplanar surfaces;[13] it is largely ineffective in generating three-dimensional structures;[11a] it is poorly suited for introducing specific chemical functionalities; it is directly applicable to only a limited set of materials used as photoresists;[14] and it integrates well with semiconductor materials, but not necessarily with glass, plastics, ceramics, or carbon. These limitations suggest the need for alternative microfabrication techniques. The development of practical methods capable of generating structures smaller than 100 nm for a range of materials represents a major task, and is one of the greatest technical challenges now facing microfabrication.[11, 12]

A number of non-photolithographic techniques have been demonstrated for fabricating (and in some cases for manufacturing) high-quality microstructures and nanostructures (Table 2).[15–38] This review will focus on the soft lithographic techniques that we are currently exploring: microcontact printing (μCP),[34] replica molding (REM),[35] microtransfer molding (μTM),[36] micromolding in capillaries (MIMIC),[37] and solvent-assisted micromolding (SAMIM).[38] Collectively, we call these techniques "soft lithography",[33] because in each case an elastomeric stamp or mold is the key element that transfers the pattern to the substrate and, more broadly, because each uses flexible organic molecules and materials rather than the rigid inorganic materials now commonly used in the fabrication of microelectronic systems (Table 3).

Table 2. Non-photolithographic methods for micro- and nanofabrication.

Method	Resolution[a]	Ref.
injection molding	10 nm	[15, 16]
embossing (imprinting)	25 nm	[17, 18]
cast molding	50 nm	[19, 20]
laser ablation	70 nm	[21, 22]
micromachining with a sharp stylus	100 nm	[23]
laser-induced deposition	1 μm	[24]
electrochemical micromachining	1 μm	[25]
silver halide photography	5 μm	[26]
pad printing	20 μm	[27]
screen printing	20 μm	[28]
ink-jet printing	50 μm	[29, 30]
electrophotography (xerography)	50 μm	[31]
stereolithography	100 μm	[32]
soft lithography		[33]
microcontact printing (μCP)	35 nm	[34, 84f]
replica molding (REM)	30 nm	[35]
microtransfer molding (μTM)	1 μm	[36]
micromolding in capillaries (MIMIC)	1 μm	[37]
solvent-assisted micromolding (SAMIM)	60 nm	[38]

[a] The lateral dimension of the smallest feature that has been generated. These numbers do not represent ultimate limits.

Soft lithography generates micropatterns of self-assembled monolayers (SAMs)[39] by contact printing, and also forms microstructures in materials by embossing (imprinting)[17, 18] and replica molding.[19, 20] Figure 3 shows the general procedure for soft lithography in a technique we call "rapid prototyping" and whose components we describe in Section 2.5. The strength of soft lithography is in replicating rather than fabricating the master, but rapid prototyping and

Table 3. Comparison of photolithography to soft lithography.

	Photolithography	Soft lithography
definition of patterns	rigid photomask (patterned Cr supported on a quartz plate)	elastomeric stamp or mold (a PDMS block patterned with relief features)
materials that can be patterned directly	photoresists (polymers with photosensitive additives)	photoresists[e]
	SAMs	SAMs[a] unsensitized polymers[b–e] (epoxy, PU, PMMA, ABS, CA, PS, PE, PVC)[f] polymer precursors[c, d] (of carbon materials and ceramics) polymer beads[d] conducting polymers[d] colloidal materials[a, d] sol–gel materials[c, d] organic and inorganic salts[d] biological macromolecules[d]
current limits to resolution	ca. 250 nm	see Table 2
minimum feature size	ca. 100 nm (?)	10 (?) – 100 nm

[a] μCP. [b] REM. [c] μTM. [d] MIMIC. [e] SAMIM. [f] PU: polyurethane; PMMA: poly(methyl methacrylate); ABS: poly(acrylonitrile-butadiene-styrene); CA: cellulose acetate; PS: polystyrene; PE: polyethylene; PVC: poly(vinyl chloride).

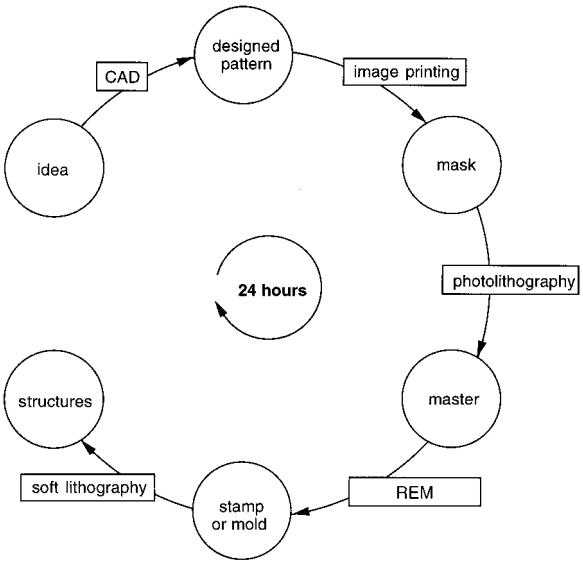

Figure 3. The rapid prototyping procedure for soft lithography. The pattern is composed and transferred to a CAD file, and printed on a transparent sheet of polymer with a commercial image setter. This patterned sheet is used in contact photolithography to prepare a master in a thin film of photoresist; a negative replica of this master in an elastomer becomes the stamp or mold for soft lithography. The overall procedure from design to stamp takes less than 24 hours to complete.

the ability to deform the elastomeric stamp or mold give it unique capabilities even in fabricating master patterns. Soft lithographic techniques require remarkably little capital investment and are procedurally simple: They can often be carried out in the ambient laboratory environment. They are not subject to the limitations set by optical diffraction and optical transparency (the edge definition is set, in principle, by van der Waals interactions and, in practice, by the properties of the materials involved), and they provide alternative routes to structures that are smaller than 100 nm without the need for advanced lithographic techniques. They also offer access to new types of surfaces, optical structures, sensors, prototype devices, and systems that could be difficult to fabricate by photolithographic procedures. Our aim in this review is to explain and examine the principles, processes, materials, and limitations of this new class of patterning techniques, and to describe their ability to form patterns and structures of a wide variety of materials with features that range from nanometers to micrometers in size.

2. Key Strategies of Soft Lithography

2.1. Self-Assembly

The obvious technical challenges to extending current photolithography to features that are smaller than 100 nm make it possible to at least consider radically new approaches to microfabrication. Both chemistry and biology can help in the development of new methodologies for microfabrication through contributions of a surprisingly broad range, both practical and conceptual. Among the conceptually new strategies offer possible routes to both smaller features and lower costs, self-assembly has been the most fully explored and is closest to practical realization.[40]

Self-assembly is the spontaneous organization of molecules or objects into stable, well-defined structures by noncovalent forces.[40] The key idea in self-assembly is that the final structure is close to or at thermodynamic equilibrium; it therefore tends to form spontaneously and to reject defects. Self-assembly often provides routes to structures having greater order than can be reached in non-self-assembling structures. The final structure is predetermined by the characteristics of the initial subunits: The information that determines the final structure is coded in the structures and properties of the subunits (e.g., shapes and surface functionalities). Self-assembly is ubiquitous in nature:[41] Processes such as folding of proteins and tRNAs as well as formation of the DNA double helix serve as biological illustrations of the potential of self-assembly in microfabrication. Various strategies of self-assembly have been developed and employed to fabricate two- and three-dimensional structures with dimensions ranging from molecular, through mesoscopic, to macroscopic sizes.[42–45]

2.2. Self-Assembled Monolayers

Self-assembled monolayers (SAMs) are the most widely studied and best developed examples of nonbiological, self-assembling systems.[39, 46] They form spontaneously by chemisorption and self-organization of functionalized, long-chain organic molecules onto the surfaces of appropriate substrates. SAMs are usually prepared by immersing a substrate in the solution containing a ligand that is reactive toward the surface, or by exposing the substrate to the vapor of the reactive species. Table 4 lists a number of systems known to give SAMs;[47–65] new systems are still being developed.

The best characterized systems of SAMs are alkanethiolates $CH_3(CH_2)_nS^-$ on gold (Figure 4).[47] Alkanethiols chemisorb spontaneously on a gold surface from solution and form adsorbed alkanethiolates. This process is assumed to occur with loss of dihydrogen; the fate of the hydrogen atom is still

Table 4. Substrates and ligands that form SAMs.

Substrate	Ligand or Precursor	Binding	Ref.
Au	RSH, ArSH (thiols)	RS–Au	[39, 46, 47]
Au	RSSR′ (disulfides)	RS–Au	[39, 46, 48]
Au	RSR′ (sulfides)	RS–Au	[39, 46, 49]
Au	RSO_2H	RSO_2–Au	[50]
Au	R_3P	R_3P–Au	[51]
Ag	RSH, ArSH	RS–Ag	[39, 52]
Cu	RSH, ArSH	RS–Cu	[39, 53]
Pd	RSH, ArSH	RS–Pd	[39, 54]
Pt	RNC	RNC–Pt	[39, 55]
GaAs	RSH	RS–GaAs	[56]
InP	RSH	RS–InP	[57]
SiO_2, glass	$RSiCl_3$, $RSi(OR')_3$	siloxane	[39, 46, 58]
Si/Si–H	$(RCOO)_2$ (neat)	R–Si	[59]
Si/Si–H	$RCH{=}CH_2$	RCH_2CH_2Si	[60]
Si/Si–Cl	RLi, RMgX	R–Si	[61]
metal oxides	RCOOH	$RCOO^- \cdots MO_n$	[62]
metal oxides	RCONHOH	$RCONHOH \cdots MO_n$	[63]
ZrO_2	RPO_3H_2	$RPO_3^{2-} \cdots Zr^{IV}$	[64]
In_2O_3/SnO_2 (ITO)	RPO_3H_2	$RPO_3^{2-} \cdots M^{n+}$	[65]

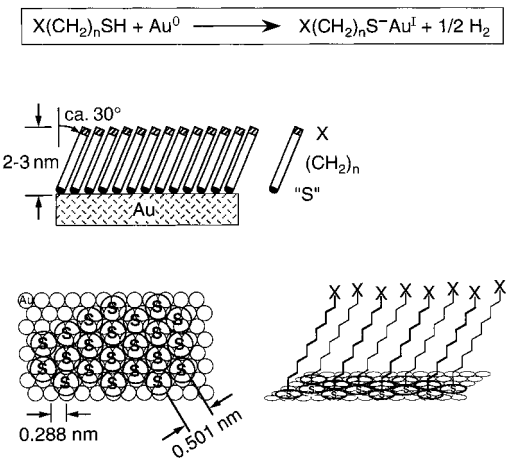

Figure 4. Representation of a highly ordered monolayer of alkanethiolate formed on a gold surface. The sulfur atoms form a commensurate overlayer on Au(111) with a $(\sqrt{3}\times\sqrt{3})R30^\circ$ structure, whose thickness is determined by the number of methylene groups (n) in the alkyl chain. The surface properties of the monolayer can be easily modified by changing the head group X. The alkyl chains $(CH_2)_n$ extend from the surface in a nearly all-*trans* configuration. On average they are tilted approximately 30° from the normal to the surface to maximize the van der Waals interactions between adjacent methylene groups.

not established. Sulfur atoms bonded to the gold surface bring the alkyl chains into close contact; these contacts freeze out configurational entropy and lead to an ordered structure. For carbon chains of up to approximately 20 atoms, the degree of interaction in a SAM increases with the density of molecules on the surface and the length of the alkyl backbones. Only alkanethiolates with $n>11$ form the closely packed and essentially two-dimensional organic quasi-crystals supported on gold that characterize the SAMs most useful in soft lithography.[46d] The formation of ordered SAMs on gold from alkanethiols is a relatively fast process: Highly ordered SAMs of hexadecanethiolate on gold can be prepared by immersing a gold substrate in a solution of hexadecanethiol in ethanol (ca. 2 mM) for several minutes, and formation of SAMs during microcontact printing may occur in seconds. This ability to form ordered structures rapidly is one of the factors that ultimately determine the success of microcontact printing.

The structures and properties of SAMs from alkanethiolates on gold have been examined using a number of techniques (Table 5).[66–82] It is generally accepted that sulfur atoms form a $(\sqrt{3}\times\sqrt{3})R30^\circ$ overlayer on the Au(111) surface (see Figure 4). Optical and diffraction techniques can only reveal the level of average order in SAMs (i.e., the dominant lattices and their dimensions) over the probed area (typically a few square millimeters). Recent STM studies show that these systems are heterogeneous and structurally complex: The alkyl chains may form a "superlattice" at the surface of the monolayer, that is, a lattice with a symmetry and dimension different from that of the underlying hexagonal lattice formed by sulfur atoms.[46d] These results indicate that the order in the top part of SAMs is not dictated solely by the sulfur atoms directly bonded to the gold surface, but also depends strongly on the intermolecular interactions between the alkyl backbones. When alkanethiolates are terminated in head groups other than methyl, it becomes even more complicated to predict and determine the structures of the SAMs.

Table 5. Techniques for characterizing SAMs of alkanethiolates on gold.

Property of SAMs	Technique	Ref.
structure and order	scanning probe microscopy	[66, 67]
	STM, AFM, LFM	[135]
	infrared spectroscopy	[39e, 68]
	low-energy helium diffraction	[69]
	X-ray diffraction	[70]
	transmission electron diffraction	[71]
	surface Raman scattering	[72]
	sum frequency spectroscopy (SFS)	[73]
composition	X-ray photoelectron spectroscopy (XPS)	[74]
	temperature programmed desorption (TPD)	[75]
	mass spectrometry (MS)	[76]
wettability	contact angle	[77]
thickness	ellipsometry	[78]
coverage and/or	quartz crystal microbalance (QCM)	[79]
degree of perfection	surface acoustic wave (SAW) device	[80]
	electrochemical methods	[81]
defects	STM and AFM	[66, 67]
	wet etching	[82]

SAMs of alkanethiolates on gold exhibit many of the features that are most attractive about self-assembling systems: ease of preparation, density of defects low enough to be useful in many applications, good stability under ambient laboratory conditions, practicality in technological applications, and amenability to controlling interfacial properties (physical, chemical, electrochemical, and biochemical) of the system. As a result, SAMs are excellent model systems for studies on wetting, adhesion, lubrication, corrosion, nucleation, protein adsorption, and cell attachment.[46, 83] SAMs are also well suited as ultrathin resists or passivating layers for fabrication of patterns and structures with lateral dimensions in the nanometer to micrometer range.

Patterning SAMs in the plane of the surface has been achieved by a wide variety of techniques (Table 6).[84–104] Each technique has advantages and disadvantages. Only micro-

Table 6. Techniques that have been used for patterning SAMs.

Technique	SAMs	Resolution[a]	Ref.
microcontact printing (μCP)			[84]
	RSH/Au	35 nm	[34, 84f, 85]
	RSH/Ag	100 nm	[86]
	RSH/Cu	500 nm	[87]
	RSH/Pd	500 nm	[88]
	RPO_3H_2/Al	500 nm	[89]
	siloxane/SiO_2	500 nm	[90, 145]
photooxidation	RSH/Au	10 μm	[91]
photo-cross-linking	RSH/Au	10 μm	[92]
photoactivation	RSH/Au	10 μm	[93]
	siloxane/glass	10 μm	[94]
photolithography/plating	siloxane/SiO_2	500 nm	[95]
electron-beam writing	RSH/Au	75 nm	[96]
	RSH/GaAs	25 nm	[97]
	siloxane/SiO_2	5 nm	[98]
focused ion beam writing	RSH/Ag	10 μm	[99]
neutral metastable atom writing	RSH/Au	70 nm	[100]
	siloxane/SiO_2	70 nm	[101]
SPM lithography	RSH/Au	10 nm	[84f, 102]
micromachining	RSH/Au	100 nm	[23, 103]
micropen writing	RSH/Au	10 μm	[104]

[a] The lateral dimension of the smallest feature that has been generated.

contact printing will be discussed in this review since it is the one that seems to offer the most interesting combination of convenience and new capability.

2.3. Contact Printing, Replica Molding, and Embossing

Contact printing is an efficient method for pattern transfer.[105] A conformal contact between the stamp and the surface of the substrate is the key to its success. Printing has the advantage of simplicity and convenience: Once the stamp is available, multiple copies of the pattern can be produced using straightforward experimental techniques. Printing is an additive process; the waste of material is minimized. Printing also has the potential to be used for patterning large areas. Although contact printing is most suitable for two-dimensional fabrication, it has also been used to generate quasi-three-dimensional structures through combination with other processes such as metal plating.[106]

Replica molding duplicates the information—for example, the shape, the morphology, and the structure—present in a master. It is a procedure that accommodates a wider range of materials than does photolithography. It also allows duplication of three-dimensional topologies in a single step, whereas photolithography is not able to replicate such structures. It has been used for the mass production of surface relief structures such as diffraction gratings,[107] holograms,[108] compact disks (CDs),[19, 20] and microtools.[109] Replica molding with an appropriate material (usually in the form of a precursor) enables highly complex structures in the master to be faithfully duplicated into multiple copies with nanometer resolution in a reliable, simple, and inexpensive way.[110–112] The fidelity of replica molding is determined by van der Waals interactions, wetting, and kinetic factors such as filling of the mold. These physical interactions should allow more accurate replication of features that are smaller than 100 nm than does photolithography, which is limited by optical diffraction.[10]

Embossing is another cost-effective, high-throughput manufacturing technique that imprints microstructures in thermoplastic materials.[17, 18] The manufacturing of CDs based on imprinting in polycarbonate with nickel masters[17a] and of holograms by imprinting in SURPHEX photopolymer (DuPont) with fused quartz masters[17f] are two typical examples of large-volume commercial applications of this technique. Until recently embossing had not been seriously developed as a method for fabricating and manufacturing structures of semiconductors, metals, and other materials used in microelectronic circuitry. The beautiful work by Chou et al. showed that embossing can be used to make features as small as 25 nm in silicon, and has attracted attention to the potential of this kind of patterning technique.[18]

We are extending the capability of these patterning techniques by bringing new approaches and new materials into these areas. In particular, a combination of self-assembly (especially of self-assembled monolayers) and pattern transfer using elastomeric stamps, molds, or masks constitutes the basis of soft lithographic methods.[33] It complements photolithography in a number of aspects and provides a wide range of new opportunities for micro- and nanofabrication.

2.4. Elastomeric Stamps and Molds

An elastomeric stamp, mold, or mask having relief structures on its surface is the key element of soft lithography.[33–38] It is usually prepared by replica molding (Figure 5) by casting

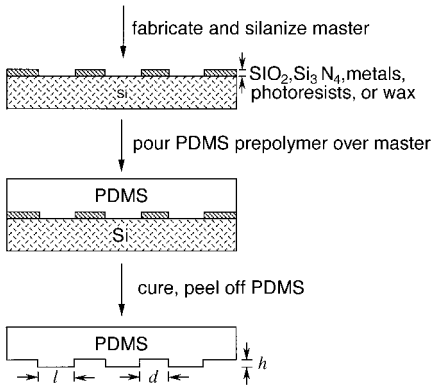

Figure 5. Schematic illustration of the procedure for casting PDMS replicas from a master having relief structures on its surface. The master is silanized by exposure to $CF_3(CF_2)_6(CH_2)_2SiCl_3$ vapor (ca. 0.5 h); each master can be used to fabricate more than 50 PDMS replicas. Representative ranges of values for h, d, and l are 0.2 – 20, 0.5 – 200, and 0.5 – 200 μm, respectively.

the liquid prepolymer of an elastomer against a master that has a patterned relief structure in its surface. The elastomer we used in most demonstrations is poly(dimethylsiloxane) (PDMS),[113] for example, Sylgard 184 from Dow Corning. We and other groups have also used other elastomers such as polyurethanes, polyimides, and cross-linked Novolac resin (a phenol formaldehyde polymer).[84, 85]

Several properties of PDMS are instrumental in the formation of high-quality patterns and structures in soft lithography. First, PDMS is an elastomer and conforms to the surface of the substrate over a relatively large area. PDMS is deformable enough such that conformal contact can even be achieved on surfaces that are nonplanar on the micrometer scale.[114] The elastic characteristic of PDMS also allows it to be released easily, even from complex and fragile structures. Second, PDMS provides a surface that is low in interfacial free energy (ca. 21.6×10^{-3} J m^{-2}) and chemically inert:[113] Polymers being molded do not adhere irreversibly to or react with the surface of PDMS. Third, PDMS is homogeneous, isotropic, and optically transparent down to about 300 nm:[115] UV cross-linking of prepolymers that are being molded is possible. It has been used to construct elastomeric optical devices for adaptive optics[116–119] and to fabricate photomasks for use in UV photolithography[120] and contact phase-shift photolithography.[121] Fourth, PDMS is a durable elastomer. We used the same stamp up to about 100 times over a period of several months without noticeable degradation in performance.[85] Fifth, the surface properties of PDMS can be readily modified by treatment with plasma followed by the formation of SAMs (Figure 6) to give appropriate interfacial interactions with materials that themselves have a wide range of interfacial free energies.[122]

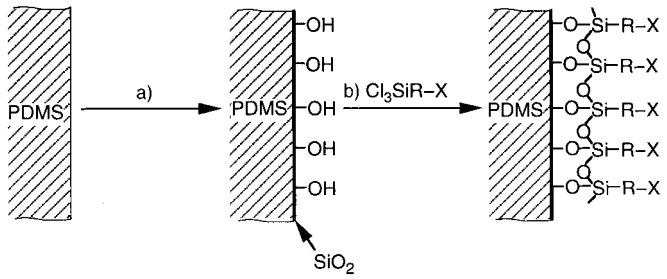

Figure 6. Schematic procedure for the modification of the PDMS surface. a) Treatment with an O_2 plasma; b) reaction with silyl chloride vapor. Different terminal groups X of the SAMs give different interfacial properties.[122]

The elastomeric character of PDMS is also the origin of some of the most serious technical problems that must be solved before soft lithography can be used in forming complex patterned structures (Figure 7). First, gravity, adhesion and

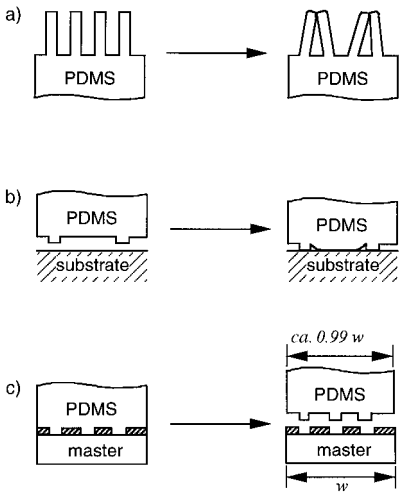

Figure 7. Schematic illustration of possible deformations and distortions of microstructures in the surfaces of elastomers such as PDMS. a) Pairing, b) sagging, c) shrinking.

capillary forces[123] exert stress on the elastomeric features and cause them to collapse and generate defects in the pattern that is formed.[124] If the aspect ratio of the relief features is too large, the PDMS microstructures fall under their own weight or collapse owing to the forces typical of inking or printing of the stamp. Delamarche et al. showed that the aspect ratios (l/h, Figure 5) of the relief structures on PDMS surfaces had to be between about 0.2 and 2 in order to obtain defect-free stamps.[124] They also found that collapsed parallel lines in PDMS could be restored by washing the stamp with sodium dodecylsulfate (SDS, ca. 1 % in water) followed by rinsing with heptane. Second, when the aspect ratios are too low, the relief structures are not able to withstand the compressive forces typical of printing and the adhesion between the stamp and the substrate; these interactions result in sagging. This deformation excludes soft lithography for use with patterns in which features are widely separated ($d \geq 20h$, Figure 5), unless nonfunctional "posts" can be introduced into the designs to support the noncontact regions. Third, achieving accurate registration without distorting the multilayer fabrication process is substantially more difficult with a flexible elastomer than with a rigid material. There are several other disadvantages that may limit the performance of PDMS for certain types of applications. For example, PDMS shrinks by a factor of about 1 % upon curing,[125] and PDMS can be readily swelled by nonpolar solvents such as toluene and hexane.[113, 126] We and other groups are beginning to address these problems associated with elastomeric materials: We recently found that we could use the Moiré technique to determine distortions of PDMS stamps or molds during soft lithography, and a method was identified for limiting the maximum distortions to less than 1 μm over areas of about 1 cm^2.[127] We believe that we will find solutions for most of these problems in the future by using new materials, new designs, and new configurations.

2.5. Masters and Rapid Prototyping

The utility of soft lithographic techniques is often limited by the availability of appropriate masters. In general, the master used to cast the PDMS stamp or mold is fabricated using microlithographic techniques such as photolithography[84] or micromachining,[128] or from available relief structures such as diffraction gratings or TEM grids.[129] Photolithography seems to be the most convenient method for generating complex patterns. Chrome masks are commercially available, but they are expensive (ca. $200 per square inch for features larger than 5 μm and ca. $500 per square inch for features between 1 and 5 μm). The time and expense involved in generating chrome masks are significant barriers to the use of photolithography by chemists and biologists. These barriers have also limited the development of soft lithography, and inhibited the use of microfabrication in a number of areas.

Recently we[130] and other groups[131] developed a system that allows fabrication of masters having feature sizes that are greater than or equal to 20 μm rapidly and at low cost (see Figure 3). In this technique we draw patterns using computer programs such as Freehand or AutoCAD and print them directly onto polymer sheets with a commercial laser-assisted image-setting system (e.g., Herkules PRO, resolution of 3387 dpi (dots per inch), Linotype-Hell Company, Hauppauge, NY). With this method photomasks, transparent polymeric sheets patterned with microstructures of black ink, can be made in a few hours at a cost of about $1 per square inch. Although these masks do not have the durability and dimensional stability required for use in the manufacturing of microelectronic devices, they are suitable for the rapid production of simple patterns that are well suited for prototyping microfluidic, microoptical, and microanalytical systems as well as for sensors.[5–9, 130] After the patterns on these polymer films are transferred into films of photoresists coated on silicon substrates using photolithography and developing, the resulting patterns can serve as masters to make the required PDMS stamps. Rapid prototyping allows the production of substantial numbers of simple microstructures rapidly and inexpensively. By combining this method with soft lithographic techniques, we can fabricate patterned

microstructures of polymers and metals within 24 hours after the design is completed. At present, the smallest feature size that can be achieved directly using this procedure is about 20 μm, a value that is limited by the resolution (ca. 3387 dpi) of the image-setting system. It should be possible to generate smaller features by using printers with higher resolutions. We believe that rapid prototyping paves the way for expanded use of microfabrication in chemistry and biology, especially when patterns may be complex but require only modest feature sizes.

3. Microcontact Printing

3.1. Principles of Microcontact Printing

Microcontact printing (μCP) is a flexible, non-photolithographic method that routinely forms patterned SAMs containing regions terminated by different chemical functionalities with submicron lateral dimensions.[84] The procedure is remarkably simple (Figure 8). An elastomeric PDMS stamp is used to transfer molecules of the "ink" to the surface of the substrate by contact. After printing, a different SAM can be formed on the underivatized regions by washing the patterned substrate with a dilute solution containing the second molecule. Microcontact printing was first demonstrated for SAMs of alkanethiolates on gold.[34] Its success relies on the rapid reaction of alkanethiols on gold and on the "autophobicity" of the resulting SAMs.[132] An exceptionally thoughtful STM study by Larsen et al. showed that for μCP with solutions of dodecanethiol in ethanol with concentrations greater than or equal to 10 mM, a contact time of longer than 0.3 s was enough to form highly ordered SAMs on Au(111) that are indistinguishable from those formed by adsorption from solution (Figure 9).[80f, 133] For μCP with hexadecanethiol (ca. 2 mM in ethanol), a contact time of about 10–20 s is usually used.[84]

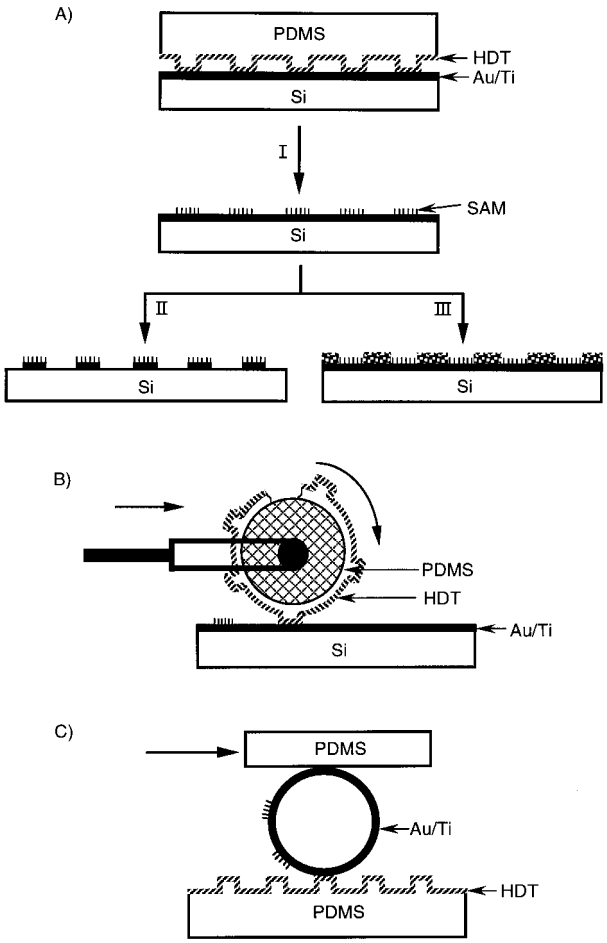

Figure 8. Schematic illustration of procedures for μCP of hexadecanethiol (HDT) on a gold surface: A) printing on a planar surface with a planar stamp (I: printing of the SAM, II: etching, III: deposition);[84] B) large-area printing on a planar surface with a rolling stamp;[147] C) printing on a nonplanar surface with a planar stamp.[149] After the "ink" (ca. 2 mM HDT in ethanol) was applied to the PDMS stamp with a cotton swab, the stamp was dried in a stream of N_2 (ca. 1 min) and then brought into contact with the gold surface (ca. 10–20 s).

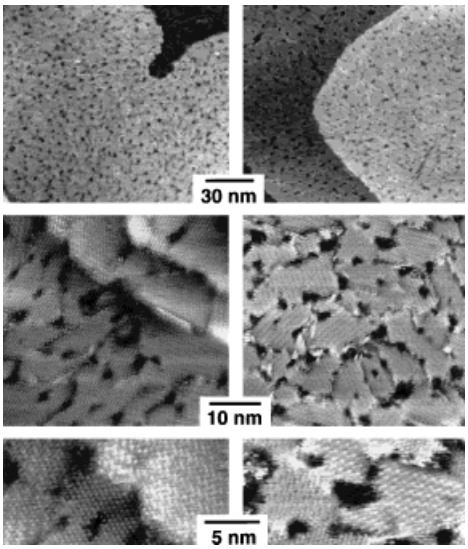

Figure 9. Comparison of STM images of SAMs of dodecanethiol (DDT) on Au(111) formed by μCP (left) and by adsorption from solution (right). The μCP was carried out with a solution of DDT in ethanol (ca. 100 mM) as the "ink" (the stamp was in contact with the gold surface for about 10 s); in the case of adsorption from solution the gold surface was equilibrated with a solution of DDT in ethanol (1 mM) for about 18 h (taken from Larsen et al.[133]).

Patterned SAMs formed by μCP can be visualized using a range of techniques such as scanning electron microscopy (SEM),[134] scanning probe microscopy (SPM),[135] secondary ion mass spectrometry (SIMS),[136] condensation figures (CFs),[136] and surface-enhanced Raman microscopy.[86b] Figure 10 compares the pattern in an original master with that of a SAM of hexadecanethiolate on gold formed by μCP with a PDMS stamp cast from this master. Figure 11 shows lateral force microscopy (LFM) images of a test pattern of SAMs of hexadecanethiolate on gold.[135b] The patterned SAMs of hexadecanethiolate formed by μCP seem to have an edge roughness less than about 50 nm.

We and other groups have extended μCP to a number of other systems of SAMs (see Table 6). The most useful systems are patterned SAMs of alkanethiolates on evaporated thin films of gold and silver, because both systems give highly ordered monolayers. Gold is interesting since it is widely used

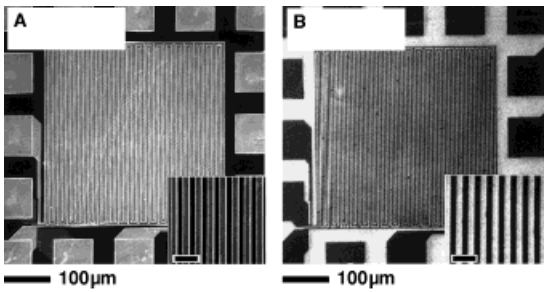

Figure 10. SEM images (at two different magnifications) of A) a master and B) the pattern of a SAM of HDT on gold formed by μCP (contact time ca. 10 s) with a PDMS stamp cast from this master. A planar PDMS stamp was used. The contrast in the image of the master (A) resulted from different heights and/or materials between regions. The dark regions on the SAM-patterned surface in image B represent the SAM of HDT, and the light regions underivatized gold. The scale bars in the insets correspond to 10 μm.

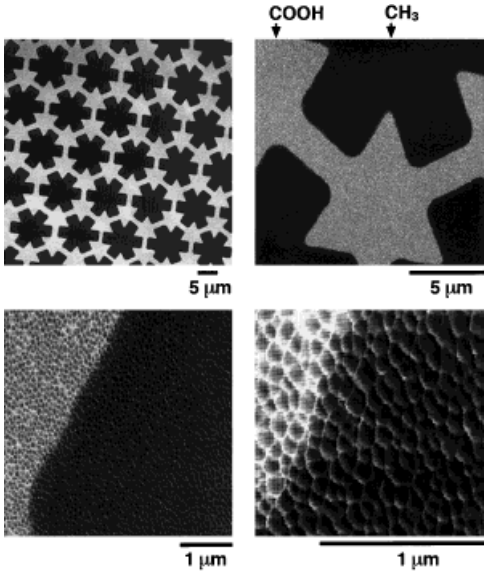

Figure 11. LFM images (at four different magnifications) of a gold surface patterned with SAMs terminated in different head groups. The surface was printed in HDT; the remaining regions were then derivatized with $HS(CH_2)_{15}COOH$ by immersing the patterned sample in a solution containing the second thiol. Relatively high frictional forces between the probe and the surface were detected in regions covered with a COOH-terminated SAM (light), and relatively low frictional forces were measured over regions covered with a CH_3-terminated SAM (dark).[135b]

as the material for electrodes in many applications,[137] and it is compatible with microelectronic devices based on GaAs (but not on silicon).[138] Silver is attractive because it is more convenient to etch than gold: Silver is chemically more reactive than gold and therefore dissolves more rapidly in most etchants;[86] the level of defects in SAMs of alkanethiolates on silver also seems to be lower than on gold.[86] Furthermore, silver is an excellent electrical and thermal conductor.[139] The system of siloxanes on HO-terminated surfaces is less tractable and usually gives disordered SAMs and in some cases submonolayers or multilayers.[140]

Patterned SAMs can be used as ultrathin resists in selective wet etching[84, 141] or as templates to control the wetting, dewetting, nucleation, growth, and deposition of other materials (Figure 8A, II and III).[142–145] They have also been used as supports to control both azimuthal and polar orientations of nematic liquid crystals (LCs).[146] The smallest features generated to date with a combination of μCP and selective etching are trenches etched in gold with lateral dimensions of approximately 35 nm.[84f] The minimum size of features that can be fabricated by μCP has still not been completely defined. Because the SAMs are only 1–3 nm thick, there is little loss in edge definition due to the thickness of the resist; the major determinants of edge resolution seem to be the fidelity of the contact printing and the anisotropy in the etching of the underlying metal. Absorbates on the surface of the substrate, the roughness of the surface, and materials properties (especially the deformation and distortion) of the elastomeric stamp also influence the resolution and feature size of patterns formed by μCP. Some tailoring of the properties of the PDMS stamp or development of new elastomeric materials optimized for the regime below 100 nm will be useful.

Microcontact printing is attractive because it is simple, inexpensive, and flexible. Routine access to clean rooms is not required (at least for fabricating structures that are larger than 20 μm by rapid prototyping and similar techniques), although occasional use of these facilities is convenient for making masters. The process is inherently parallel—that is, it forms the pattern over the entire area of the substrate in contact with the stamp at the same time—and thus suitable for forming patterns over large areas ($\geq 50\,cm^2$) in a single impression (Figure 8B).[147] The elastomeric PDMS stamp and the surface chemistry for the formation of SAMs can be manipulated in a number of ways to reduce the size of features generated by μCP.[148] It can, in principle, be used for many micro- and nanofabrication tasks and is a low-cost process. In particular, it can be applied to types of patterning where optically based lithography simply fails, for example, patterning nonplanar surfaces.[149]

3.2. Patterned SAMs as Ultrathin Resists in Selective Wet Etching

SAMs do not have the durability to serve as etch masks in conventional reactive-ion etching.[150] They are, however, efficient resists for certain types of wet etchants. Table 7 summarizes selective chemical etchants that have been studied for use with patterned SAMs.[84, 141] Many other selective etches are known for these and other materials, and they remain to be explored in conjunction with SAMs.[151]

Figure 12 shows SEM images of a series of test patterns of silver that were fabricated by μCP with hexadecanethiol followed by selective etching in aqueous solutions of ferricyanide.[86a] The SAM-derivatized regions were barely attacked by the etchant within the time required to remove the bare regions. These images represent the level of complexity, perfection, and scale that can be produced *routinely* with μCP. The ability to generate arrays of microstructures of coinage metals with controlled shapes and dimensions is directly useful in fabricating arrays of microelectrodes for sensors[8] and other electrochemical devices.[137] Another application of μCP is in the preparation of gold or silver patterns to be used

Table 7. Selective etchants that have been used with patterned SAMs generated by μCP (all wet etchants were used in aqueous solutions).

Surface	SAM	Etchant (approximate pH)	Ref.
Au	RS^-	$K_2S_2O_3/K_3[Fe(CN)_6]/K_4[Fe(CN)_6]$ (14)	[84, 85, 141]
		KCN/O_2 (14)	[34, 84, 85]
		$CS(NH_2)_2/H_2O_2$ (1)	[84e, 141]
Ag	RS^-	$Fe(NO_3)_3$ (6)	[84e, 86a]
		$K_2S_2O_3/K_3[Fe(CN)_6]/K_4[Fe(CN)_6]$ (7)	[84e, 86a, 141]
		$NH_4OH/K_3[Fe(CN)_6]/K_4[Fe(CN)_6]$ (12)	[84e, 86a]
		NH_4OH/H_2O_2 (12)	[84e, 86a]
		NH_4OH/O_2 (12)	[84e, 86a]
		KCN/O_2 (14)	[84e, 86a, 141]
Cu	RS^-	$FeCl_3$/HCl (1)	[84e, 87b]
		$FeCl_3/NH_4Cl$ (6)	[84e, 87b]
		H_2O_2/HCl (1)	[84e, 87a]
GaAs	RS^-	HCl/HNO_3 (1)	[84e, 97]
Pd	RS^-	HCl/HNO_3 (1)	[88]
Al	RPO_3^{2-}	HCl/HNO_3 (1)	[89]
Si/SiO_2	$RSiO_{3/2}$[a]	HF/NH_4F (2)	[90b]
glass	$RSiO_{3/2}$[a]	HF/NH_4F (partially selective)	[90b]

[a] These SAMs are formed by contact of $RSiCl_3$ or $RSi(OCH_3)_3$ with the substrates.

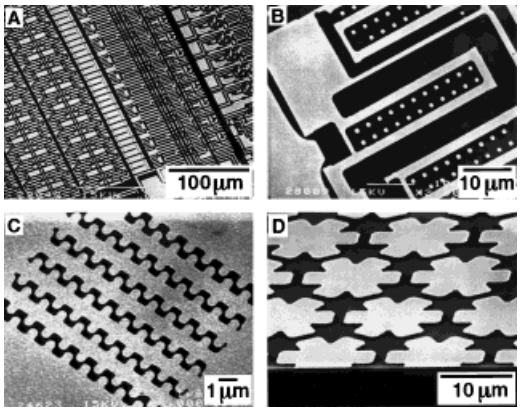

Figure 12. SEM images of test patterns on layers of silver (A, B, C: 50 nm thick; D: 200 nm thick) that were fabricated by μCP with HDT followed by chemical etching in an aqueous solution of ferricyanide. The patterns in A and B were printed with rolling stamps,[147] and those in C and D with planar stamps.[86a] The bright regions represent silver, and the dark regions Si/SiO_2 in which unprotected silver has dissolved.

as secondary masks in the etching of underlying substrates such as SiO_2, silicon, and GaAs.[152, 153] Figure 13 shows SEM images of microstructures in silicon that were fabricated by anisotropic etching of Si(100) in an aqueous solution containing KOH and 2-propanol with patterns of silver (50 nm thick) as masks.[86a, 154] The silver masks were in turn generated with a combination of μCP of hexadecanethiol and selective chemical etching.

SAMs and patterning by μCP illustrate a new approach to microfabrication. Although this combination is proving immediately useful in single-layer fabrication (e.g., sensors and microelectrode arrays), several issues remain to be solved before it can be considered for application in complex microelectronics. For example, the formation and distribution of defects in SAMs, especially under the conditions of chemical etching, must be understood. A recent study based on a method involving two-stage chemical amplification found that the density of defects in SAMs depended on the

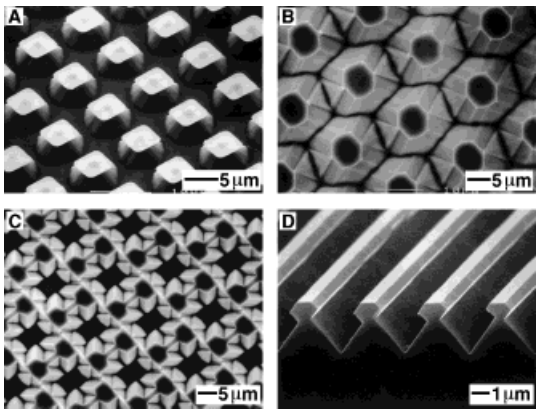

Figure 13. SEM images of silicon structures generated by anisotropic etching of Si(100) with patterned structures of silver or gold as masks.[86a, 120] The metal mask is still on the surface in A; it has been removed by immersion in aqua regia for B, C, and D. The structure in D was fabricated by a combination of shadow evaporation and anisotropic etching of Si(100).[153]

thickness of the gold layer, the length of the alkyl chain, and the conditions used for preparing the SAMs.[82] The density of defects in printed SAMs (in terms of pinholes in SAM-derivatized regions) measured using this technique was about 10^3 pits per mm^2 for 50 nm thick gold, and about 10 pits per mm^2 for 50 nm thick silver.[155] These densities are still too high to be useful for fabricating high-resolution microelectronic devices. The latter is, however, low enough that silver lines (200 nm thick and 50 μm wide) extending approximately 5 m in length are electrically continuous with no evidence of electrically significant defects.[130] The patterned microstructures fabricated using this procedure are acceptable for applications in many areas other than microelectronics, including the production of microelectromechanical systems (MEMS),[5] microanalytical systems,[6] sensors,[8] solar cells,[156] and optical components.[152b, 157]

3.3. Patterned SAMs as Passivating Layers in Selective Deposition

Through chemical control of the length of the polymethylene chain, the thickness of a SAM can be predetermined with a precision of about 0.1 nm. Organic synthesis also makes it possible to incorporate different functional groups (e.g., fluorocarbons, acids, esters, amines, amides, alcohols, nitriles, and ethers) into and/or at the termini of the alkyl chain.[39] With μCP, SAMs with different functional head groups can be organized into different patterns on a single surface and employed to control wetting, dewetting, nucleation, or deposition of other materials on this surface.[142–145]

Figures 14A and 14B shows how functionalities of SAMs influence the wetting and dewetting of liquids on SAM-patterned surfaces. These processes are determined by the minimization of free energies. They use self-assembly at two scales: the formation of SAMs at the molecular scale and the fabrication of structures of liquids at the mesoscopic scale. Figure 14A shows an optical micrograph of drops of water preferentially condensed on hydrophilic regions of a surface

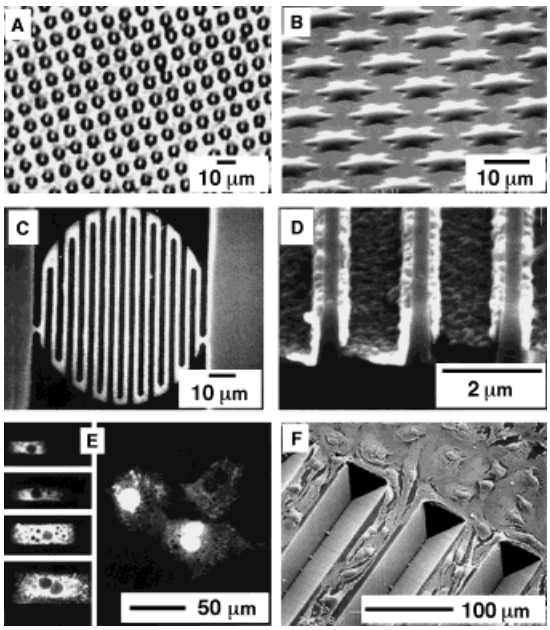

Figure 14. Demonstration of selective nucleation and deposition with patterned SAMs as templates. A) An optical micrograph of water condensed on a SAM-patterned gold surface.[142a] B) An SEM image of microstructures of polyurethane assembled by selective dewetting;[142b] only COOH-terminated regions were covered by water or polyurethane liquid. C) An SEM image of microstructures of $LiNbO_3$ on Si/SiO_2 produced with selective CVD.[145b] D) An SEM image of copper microstructures formed in silicon microtrenches with selective CVD.[145a] $LiNbO_3$ and copper only nucleated and grew on bare regions of SiO_2 underivatized by CH_3-terminated siloxane SAMs. E) Optical micrographs of hepatocytes placed on SAM-patterned (left) and bare surfaces (right).[143a] F) An SEM image of mammalian cells selectively attached to the plateaus of a contoured surface.[143b] In E and F the surfaces were derivatized by μCP in such a way that certain regions of the surface terminated in methyl groups whereas others terminated in oligo(ethylene glycol) groups. The matrix protein (fibronectin) only adsorbed to the methyl-terminated regions, and cells only attached to those regions where the matrix proteins were adsorbed.

patterned with SAMs terminated in carboxylic (COOH) and methyl groups (CH_3); no water condensed on the hydrophobic regions.[142a] Figure 14B shows an SEM image of patterned microstructures of polyurethane (PU) formed by selective dewetting.[142b] The liquid prepolymer of PU placed on the SAM-patterned surface selectively dewetted those regions derivatized with methyl groups (CH_3) and formed patterned structures on the hydrophilic regions terminated in hydroxyl groups (CH_2OH). The prepolymer was then solidified by curing under UV light. The organization of liquids into patterned arrays illustrates the use of controlled wettability in microfabrication. These patterned mcirostructures of polymers have been used as arrays of microlenses[142b] and optical waveguides.[142f]

Nuzzo et al. demonstrated selective chemical vapor deposition (CVD)[158] on Si/SiO_2 with printed SAMs of siloxanes as templates (Figures 14C, D).[145] The patterned SAMs directed the selective CVD by inhibiting nucleation: The material to be patterned only nucleated and grew on the bare regions underivatized with SAMs and formed continuous structures. This procedure could in principle be used to deposit a variety of materials selectively on many substrates without photolithography. The selective CVD of Cu may be useful in microelectronics processing, including the fabrication of thin-film interconnects (with feature sizes of ca. 0.5 – 100 μm) and selective filling of trenches and vias (representative microstructures having high aspect ratios) with feature sizes below about 1 μm.[159]

Patterned SAMs have also been used as templates to define and control the adsorption of extracellular matrix proteins and consequently the attachment of mammalian cells.[143] This technique makes it possible to place cells in predetermined locations in an array with defined shapes, sizes, and distances of separation. Figures 14E and 14F show SEM images of cells that have been selectively attached to a planar[143a] and a contoured surface,[143b] respectively. Using simple patterning procedures, it is possible to dictate the shape assumed by a cell that attaches to a surface and thus to control certain aspects of cell growth and protein secretion. This technique allows us to examine the influence of cell morphology on cell metabolism,[143d] and should be useful for applications in biotechnology that require analysis of individual cells cultured at high density and/or repeated access to cells placed in specified locations. The results of these studies may eventually shed light on complex phenomena such as contact inhibition of cell proliferation, or they may lead to new analytical systems based on arrays of cells.

3.4. Formation of Microstructures on Nonplanar Surfaces

Patterning on nonplanar surfaces has been a substantial challenge for photolithography and related techniques: even gently curved surfaces often cannot be patterned by photolithography because of limitations to depth of focus.[13] Because μCP involves conformal contact using an elastomeric stamp, it offers immediate advantages over photolithography in patterning nonplanar surfaces.[149]

Figure 8C illustrates one method for forming patterned microfeatures on surfaces of capillaries. A piece of flat PDMS stamp is used to control the movement of the capillary. Figures 15A and 15B show SEM images of test patterns of gold that were formed on gold-coated glass capillaries by μCP with hexadecanethiol followed by selective etching in an aqueous solution of cyanide.[149] They clearly show well-defined features of gold with dimensions of a few microns on capillaries with radii of curvature of about 500 μm (Figure 15A) and about 50 μm (Figure 15B). Microcontact printing can generate microstructures on planar and nonplanar surfaces with similar edge resolution. At present, there is no comparable technique for microfabrication on curved surfaces. Our recent demonstration of using electroless deposition rather than metal evaporation for preparing thin films of silver as the substrates for μCP of alkanethiols further simplifies the procedure for patterning nonplanar surfaces (even hidden surfaces such as the inside surfaces of hollow glass tubes).[114] The procedure based on μCP opens the door immediately to new types of electronic, optical, MEMS, and analytical structures including microtransformers (Figure 15C),[160] current carriers in microinductors,[160] microsprings

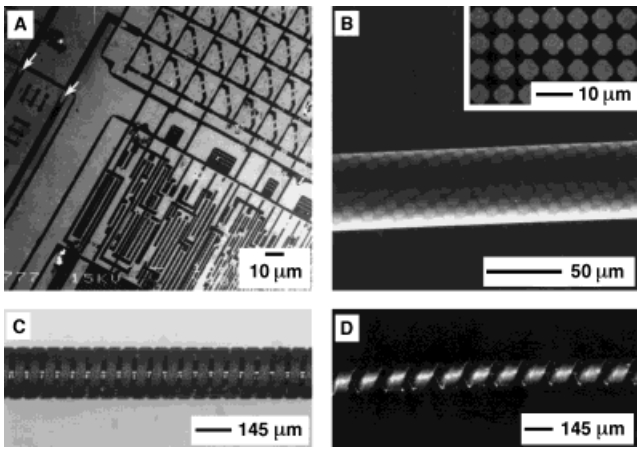

Figure 15. A, B) SEM images of test patterns of gold on curved surfaces (curvature 500 and 50 μm, respectively) that were fabricated by μCP with HDT followed by selective etching in an aqueous solution of KCN saturated with O_2.[149] C, D) Optical micrographs of a microtransformer[160] and a microspring[161] fabricated by μCP with HDT on silver (coated on the capillaries) followed by selective etching of silver and electroplating of nickel (C) and copper (D). The arrows in A indicate two defects caused by sagging.

(Figure 15 D),[161] in-fiber notch filters and Bragg gratings,[162] micro-coils for high-resolution NMR spectroscopy,[163] and intravascular stents.[164]

3.5. Microcontact Printing of Other Materials

Microcontact printing seems to be a general method for forming patterns of a variety of materials on surfaces of solid substrates through contact pattern transfer. We demonstrated μCP of protonic acids[165] and liquids containing suspended palladium colloids[106, 166] using similar procedures. Protonic acids were printed onto thin films of acid-sensitive photoresist.[167] They acted as the catalyst for the decomposition of the photoresist upon heating: Regions sensitized by acids became soluble in the basic developing solution. Colloids were also printed directly on a variety of substrates including glass, Si/SiO_2, and polymer films.[106, 166] The deposited colloids acted as catalysts for electroless deposition of metals (Figure 16). Microcontact printing of aqueous solutions containing biological molecules (e.g., proteins and enzymes) might also be possible, although formation of uniform monolayers of such materials using printing might be difficult.

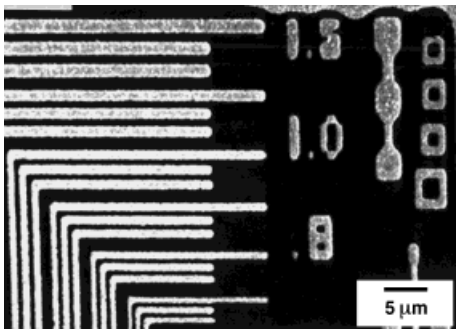

Figure 16. An SEM image of copper microstructures that were fabricated by electroless plating onto a pattern of electrocatalytic colloid particles of palladium. The palladium pattern was printed by μCP.[106]

4. Micromolding and Related Techniques

4.1. Replica Molding

Our procedure for replica molding (REM; Figure 17 A) differs from conventional procedures in the use of an elastomeric mold rather than a rigid mold.[35, 168] The elasticity

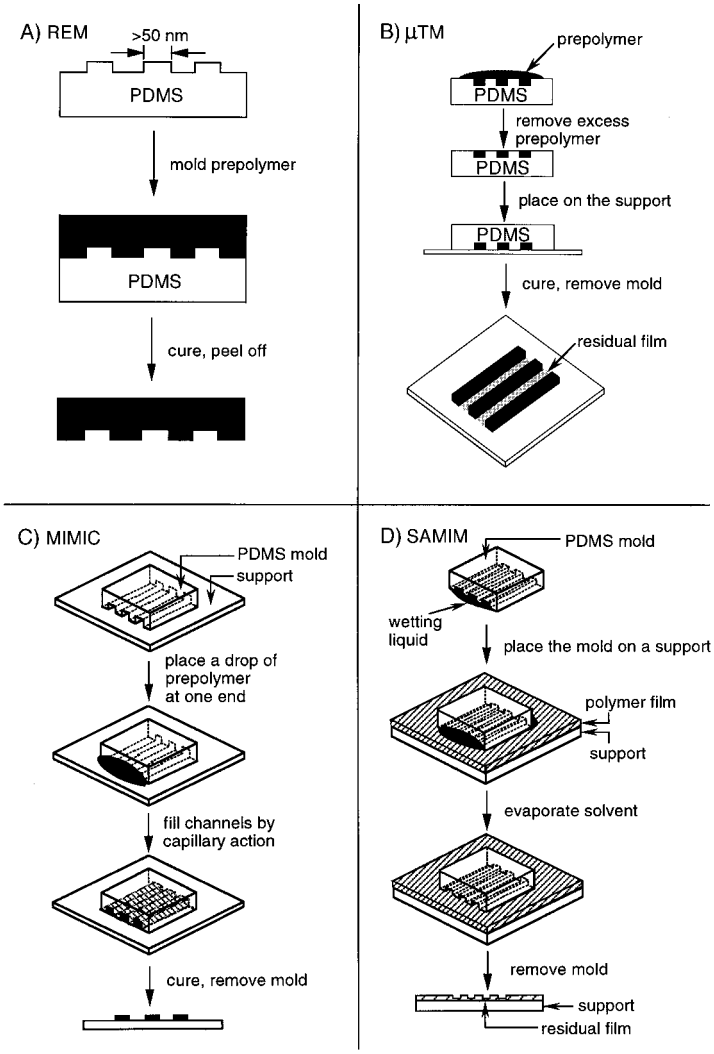

Figure 17. Schematic illustration of procedures for A) replica molding, B) microtransfer molding, C) micromolding in capillaries, and D) solvent-assisted micromolding.

and low surface energy of the elastomeric PDMS mold allows it to be released easily. An elastomeric mold also offers the opportunity to manipulate the size and shape of features present on the mold by mechanical deformation. The capability and versatility of this new procedure has been demonstrated for nanomanufacturing:[169] Conventional high-resolution nanolithographic techniques would be used to make masters, and these structures would then be duplicated into multiple copies by replica molding with organic polymers. This technique has also been adapted for the fabrication of topologically complex, optically functional surfaces that would be difficult to fabricate with other techniques.[35]

4.1.1. Nanomanufacturing

We demonstrated that replica molding against elastomeric molds is possible with a resolution on the nanometer scale.[169] Figure 18 shows AFM images of chromium structures on a

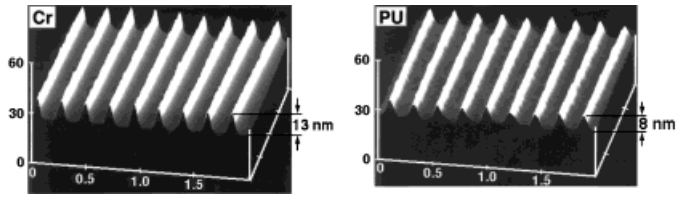

Figure 18. AFM images of chromium structures on a master and a PU replica prepared from a PDMS mold cast from this master.[169] The width is given in micrometers; the depth and height are given in nanometers.

master[170] and a PU replica prepared from a PDMS mold cast against this master. The most important feature of this replicated PU is the accuracy with which the vertical dimension is reproduced. The heights of the chromium lines on the original master were about 13 nm; the heights of the PU lines were about 8 nm. The prepolymer of PU used here shrinks less than 3% upon curing.[171] These images demonstrate that, within our ability to compare similar structures, this replica molding procedure duplicated structures within a few nanometers over substantial areas (ca. 1 mm^2).

We also monitored the quality of the replica structures generated from successive molds prepared from the same master.[169] Figure 19A shows the AFM image of gold structures on a master before it was used to cast PDMS molds; the gold master was prepared using a procedure including electron-beam writing in a resist, development of the lines, metal evaporation, and lift-off. Figure 19B shows an

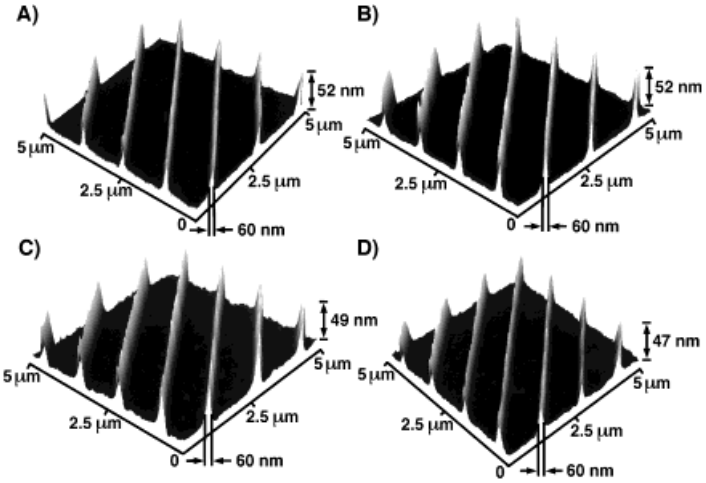

Figure 19. A, B) AFM images of gold structures on a master A) before it was used to cast PDMS molds and B) after it had been used to cast seven PDMS molds. C, D) AFM images of PU replicas produced from different PDMS molds cast from this master.[169]

AFM image of this gold master after it had been used to cast seven PDMS molds. We observed no damage to the gold master after its repeated use (ten times) to form PDMS stamps. Figures 19C and 19D show AFM images of PU replicas generated from different PDMS molds. Again, we did not observe obvious change in the quality of these nanostructures on the PU replicas. These AFM images clearly demonstrate that this procedure is able to generate multiple copies of nanostructures starting from a single master. The simplicity and low cost of this procedure suggest its potential use in nanomanufacturing.

A modification of the procedure, replica molding against an PDMS mold while it is bent mechanically, allows the fabrication of nanostructures with feature sizes smaller than those on the original master.[169] Figure 20A shows the AFM image of gold structures on another master with a feature size of about 50 nm, and Figure 20B the AFM image

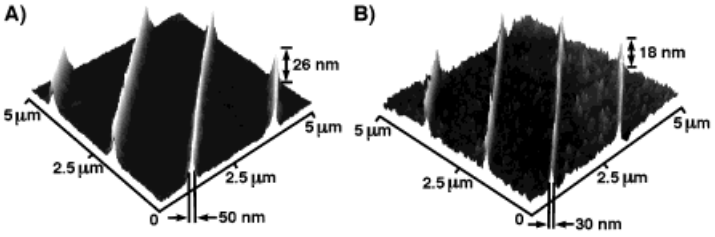

Figure 20. AFM images A) of Au structures on a master before it was used to cast PDMS molds and B) of a PU replica fabricated from a PDMS mold (cast from this master) while this mold was mechanically deformed by bending in a manner that generated narrower lines.[169]

of a PU replica duplicated from a PDMS mold (cast from this gold master) while it was bent mechanically. The dimension of the features was reduced from 50 to 30 nm in this process.

The absence of techniques that are capable of generating and manufacturing nanostructures rapidly and economically represents one current limiting step in the area of nanoscience and nanotechnology.[12] This work based on replica molding demonstrates a practical protocol for fabricating structures as small as approximately 30 nm in organic polymers, and with an accuracy in vertical dimension as small as about 5 nm. Recently, Chou et al. demonstrated a related procedure that might also be included in soft lithography: embossing or imprinting in organic polymers with rigid masters. This method generates features in thermoplastic polymers with dimensions as small as about 25 nm.[18] Related work has also been demonstrated by groups at Phillips[19a] and IBM.[19b] These demonstrations make it clear that manufacturing (i.e., fabrication of multiple copies) of nanostructures of organic polymers is a practical reality. The ability to make both positive and negative polymeric replicas and to modify the dimensions and shapes of features present on elastomeric molds by mechanical deformation adds further flexibility to this methodology. Using nanostructures to generate electronically, optically, and magnetically functional components and systems will require the development of new technologies; the present work may provide one solution to the problem of mass production of nanostructures. Lessons learned from this process will be valuable in building more versatile systems.

4.1.2. Fabrication of Complex Optical Surfaces

Replica molding against a deformed PDMS mold provides a new strategy for making topologically complex structures and optically functional surfaces.[35, 168] It allows the sizes and shapes of features present on the surface of the mold to be changed in a controlled way (by mechanical compression, bending, stretching, or a combination of these deformations) and generates complex structures from simple, regular structures on planar surfaces. The highly isotropic deformation of the PDMS mold even permits patterned microstructures to be formed with gradients in size and shape. The relief features on the PDMS mold are reconfigured by mechanical deformation, and the deformed structures are replicated by casting an UV-curable liquid PU or a thermally curable epoxy against it. The capability and feasibility of this procedure has been demonstrated by the production of[35] 1) diffraction gratings with periods smaller than the original grating used as the master to cast the PDMS mold, 2) chirped, blazed diffraction gratings on planar and curved surfaces, 3) patterned microfeatures on the surfaces of approximately hemispherical objects, and 4) arrays of rhombic microlenses.

Figure 21 summarizes the typical procedures used in replica molding against elastomeric molds under mechanical deformation.[35] Figure 21 A shows the procedure for replica molding against a PDMS mold under mechanical compression. If desired, this procedure can be repeated, using the PU replica as the starting point, to make structures more complex than

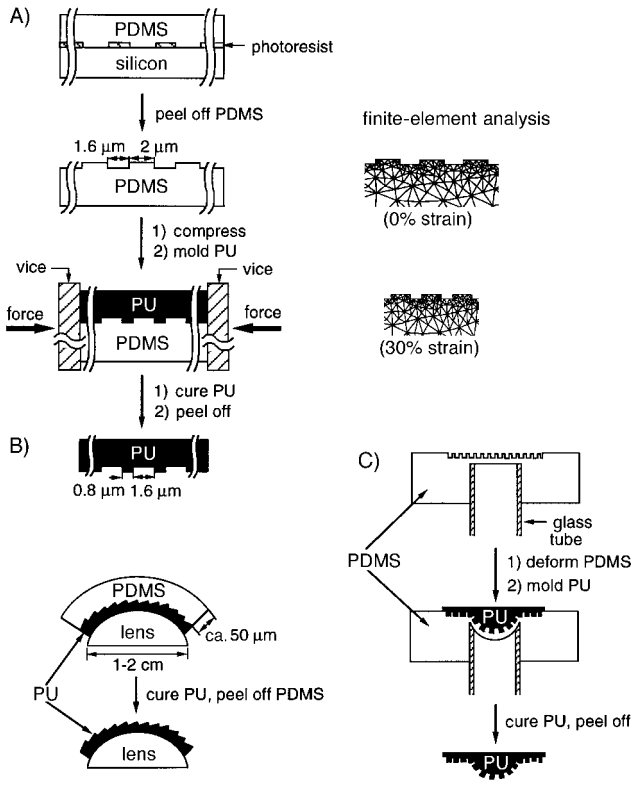

Figure 21. Schematic illustration of procedures for replica molding against elastomeric PDMS molds under A) mechanical compression, B) bending, and C) stretching.[35] The reconfigurated surfaces in PDMS are replicated with a UV-curable prepolymer of PU.

can be generated in one cycle (although with some degradation in the quality of the fabricated structures). Using a test structure of parallel lines, two cycles of compression and replication reduced the size of some features (that is, the recessed areas on the mold) from 1.6 μm to about 200 nm, and reduced the period of this test pattern from 3.6 to about 1.5 μm.[35] Figure 21 B illustrates the procedure that we used to fabricate diffraction gratings on cylindrical surfaces. A thin PDMS mold (ca. 50 μm thick) was bent to make conformal contact with a curved surface coated with a thin film of liquid PU. After curing the PU, the PDMS mold was removed to reveal the PU replica on the surface of the cylindrical substrate. Figure 21 C shows a similar procedure that was used to produce an approximately hemispherical object having micropatterned relief structures on its surface. A thin PDMS mold (ca. 1 mm thick) was mounted across the end of a hollow glass tube and deformed by applying positive or negative pressure through the tube. The resulting curved surface was then replicated in PU.

By compressing one end of the elastomeric mold more than the other, it was straightforward to fabricate a chirped diffraction grating, a grating whose period changes continuously with position.[172] More interestingly, the shape of the diffracting elements was largely preserved in this process: If we used a blazed grating as the starting master, the resulting chirped PU replica was also a blazed grating (Figure 22).[35] The period (Λ) of this chirped, blazed grating changed continuously from a value of about 1.55 to about 1.41 μm over a distance of approximetly 0.9 cm; the rate of chirping $d\Lambda/dz$ was approximately 1.6×10^{-5}. This grating was characterized in transmission at normal incidence. Figure 22 C shows the diffraction patterns (the zero-order and the two first-order peaks) of the PDMS mold, its PU replica, and the chirped PU grating. The first diffraction peak shifted continuously in position as the laser spot was scanned across the chirped grating along the z direction.

Figure 23 shows the SEM image of a hemispherical PU object with a pattern of corner cubes on its surface.[35, 168] The shape of this polymeric object can be easily tuned by changing the thickness of the PDMS mold or the applied pressure or both. We have made a range of different patterns and relief structures; the smallest feature had a size of about 1.5 μm.

4.2. Microtransfer Molding

In microtransfer molding (μTM, see Figure 17 B)[36] a drop of liquid prepolymer is applied to the patterned surface of a PDMS mold and the excess liquid is removed by scraping with a flat PDMS block or by blowing off with a stream of nitrogen. The filled mold is then placed in contact with a substrate and irradiated or heated. After the liquid precursor has cured to a solid, the mold is peeled away carefully to leave a patterned microstructure on the surface of the substrate.

Figure 24 shows SEM images of typical structures of polymers that were fabricated by μTM.[36] Microtransfer molding is capable of generating both isolated and interconnected microstructures (Figure 24 A). The most significant advantage of μTM over other microlithographic techniques is

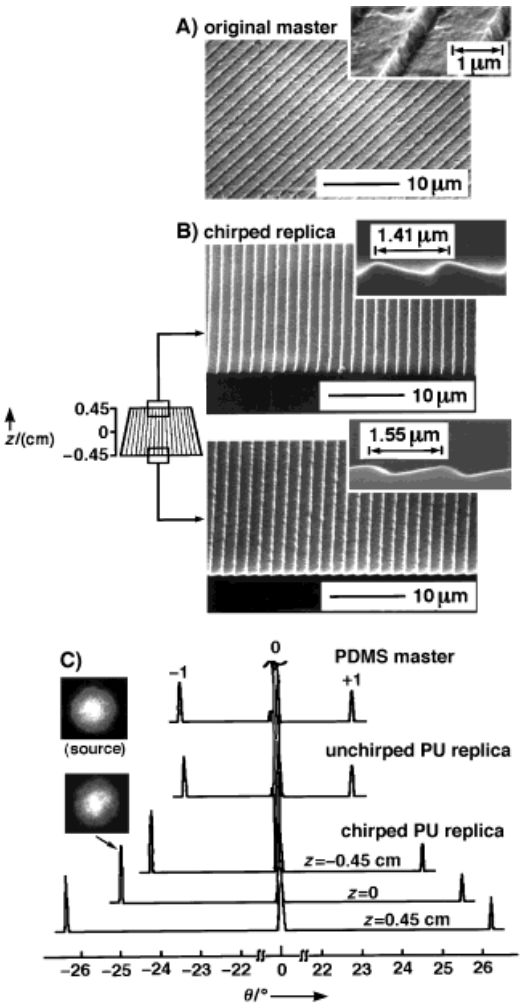

Figure 22. Cross-sectional SEM images of A) a commercial blazed diffraction grating and B) selective regions of a planar, chirped, blazed PU replica grating that was fabricated by molding against the PDMS mold while it was compressed asymmetrically. C) Diffraction patterns from the PDMS master, its PU replica, and the chirped PU grating. A He-Ne laser ($\lambda = 632.8$ nm) was used.[35]

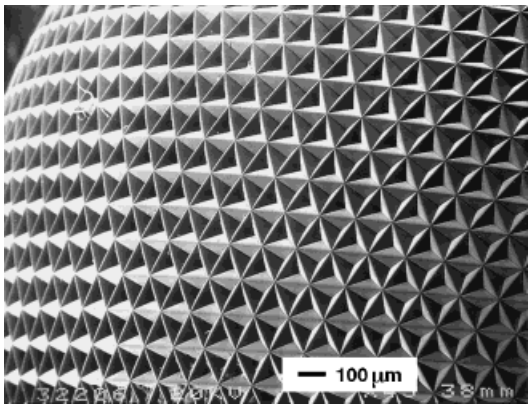

Figure 23. An SEM image of a dome-shaped object in polyurethane with patterned microstructures (corner cubes ca. 100 μm) on its surface that was formed by replica molding against a stretched PDMS mold.[35]

the ease with which it can fabricate microstructures on nonplanar surfaces, a characteristic that is essential for building three-dimensional microstructures layer by layer.

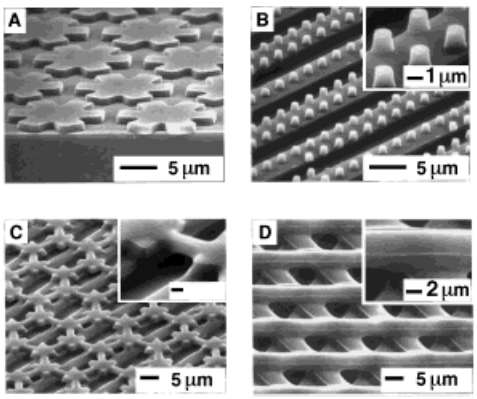

Figure 24. SEM images of polymeric microstructures fabricated by μTM:[36] A) patterned, isolated microstructures of PU on silver (one layer); B) isolated microcylinders of epoxy on 5-μm lines of epoxy supported on a glass slide (two layers); C) a continuous web of epoxy over a layer of 5-μm lines of epoxy supported on a glass slide (two layers); D) a three-layer structures on a glass slide made from a thermally curable epoxy.

Figure 24B shows microposts of thermally curable epoxy fabricated on an array of parallel lines made of the same material. Figure 24C shows a continuous polymeric web fabricated over separated polymer lines. Figure 24D shows a three-layer structure of epoxy fabricated by μTM. Analogues of these two- and three-dimensional microstructures may find potential application in integrated optics,[173] applied optics (as photonic crystals[174]), and tissue engineering.[175]

Microtransfer molding can generate microstructures over relatively large areas (ca. 3 cm^2) within a short period of time (ca. 10 min). It has been used to fabricate optical waveguides, couplers, and interferometers from organic polymers.[176] We fabricated arrays of polymeric waveguides (both single- and multimode) of 3 cm in length from thermally curable epoxies and UV-curable PU; both polymers could be pristine or doped with fluorescent dyes (e.g. rhodamine 6G).[36] An array of such waveguides could be turned into optical couplers and interferometers by tuning the separation between them; the coupling could also be controlled after fabrication by additional exposure to UV light.[176] Microtransfer molding also has the capability of forming patterned microstructures of a wide variety of other materials. Figures 25A and 25B show SEM images of microstructures of glassy carbon (an interdigitated capacitor and an optical deflector, respectively); the structures were fabricated by μTM with a polymeric precursor (a phenolic resin modified with furfuryl alcohol) followed by pyrolysis at elevated temperatures.[177] Figures 25C and 25D give SEM images of microstructures (an array of square pyramids and a free-standing membrane, respectively) of glasses fabricated from sol–gel precursors.[178] One important shortcoming of μTM in its current state of development is that microstructures fabricated on a flat surface usually have a thin film (ca. 100 nm) between the raised features. This film prevents the underlying substrate from being attacked by chemical etchants, and must be removed by reactive-ion etching with O_2 if we want to use these patterned structures of polymers as masks to control the etching of the underlying substrate. Although removing this film requires a separate

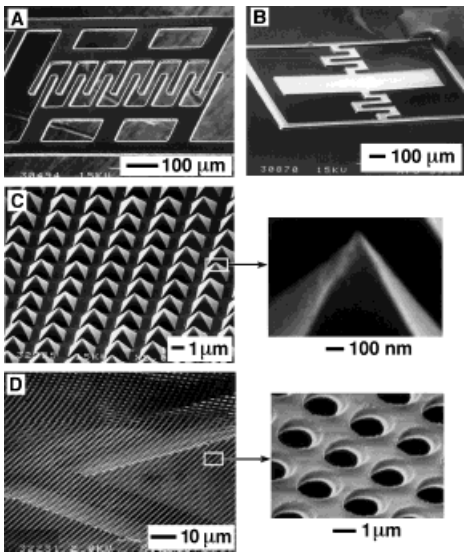

Figure 25. SEM images of A, B) microstructures of glassy carbon[177] and C, D) glasses fabricated by μTM and molding.[178] The retention of details in both procedures is very good.

step and is an inconvenience, we believe that μTM will find a broad application in microfabrication, especially for making three-dimensional microstructures.

4.3. Micromolding in Capillaries

Micromolding in capillaries (MIMIC) represents another non-photolithographic method that forms complex microstructures on both planar and curved surfaces.[37] In MIMIC (see Figure 17C) the PDMS mold is placed on the surface of a substrate and makes conformal contact with that surface; the relief structure in the mold forms a network of empty channels. When a low-viscosity liquid prepolymer is placed at the open ends of the network of channels, the liquid spontaneously fills the channels by capillary action. After filling the channels and curing the prepolymer into a solid, the PDMS mold is removed, and a network of polymeric material remains on the surface of the substrate. A variety of materials (see Table 3) have been used in this process[37] including prepolymers that are curable either with UV light or thermally,[179] precursors to carbons[177] or ceramics,[180] structural and functional polymers,[181, 182] polymer beads,[183] colloids,[184] inorganic salts,[184] sol–gel materials,[185] and biological macromolecules.[186]

Microfabrication based on MIMIC is remarkable for its simplicity and its fidelity in transferring the patterns from the mold to the polymeric structures that it forms. MIMIC is applicable to patterning a broader range of materials than is photolithography. MIMIC forms patterned structures in a single step, and patterning structures with multiple thicknesses (quasi-three-dimensional structures) is possible. The smallest features that we produced using this procedure were parallel lines with cross-sectional dimensions of about $0.1 \times 2\ \mu m^2$.[179] These dimensions were set by the PDMS molds that were available for use with this work; we have not tried molds with smaller features, and therefore the lower limit to the pattern definition that can be achieved by this technique has not been established.

MIMIC does have several limitations: 1) It requires a hydraulically connected network of capillaries; it cannot, therefore, form isolated structures or patterns on contoured surfaces. 2) Although capillary filling over a short distance (ca. 1 cm) can be achieved quickly and efficiently, the rate of filling over a large distance decreases significantly due to the viscous drag of the fluid in the capillary. 3) Since the rate of filling is proportional to the cross-sectional dimension of the capillary, the extremely slow filling of small capillaries may limit the usefulness of MIMIC in certain types of nanofabrication. Nevertheless, several groups have demonstrated that appropriate liquids could wet and fill nanometer-sized capillaries over short distances.[187, 188] 4) The forward ends of capillaries may fill incompletely if the hydraulic drag is sufficiently high.[189] Interestingly, capillaries with closed ends may fill completely if they are short; the gas in them appears to escape by diffusing into the PDMS.

4.3.1. The Principle of MIMIC

Capillary filling is a very simple and well-known phenomenon,[190] and the dynamics of wetting and spreading of liquids in capillaries has been studied systematically.[191] The flow of a liquid in a capillary occurs because of a pressure difference between two hydraulically connected regions of the liquid mass, and the direction of flow decreases this difference in pressure. In circular capillaries, the flow of a wetting liquid occurs initially in thin films that wet the capillary symmetrically; in noncircular capillaries the most rapid flow usually occurs in the corner regions.[191]

The rate of capillary filling is determined by the surface tension γ and viscosity η of the liquid, the radius of the capillary R, and the length of the filled section of the capillary z [Eq. (2); γ_{LV}, γ_{SV}, and γ_{SL} are liquid–vapor, solid–vapor, and solid–liquid interfacial free energies].[190] The rate of filling

$$\frac{dz}{dt} = \frac{R\gamma_{LV}\cos\theta}{4\eta z} = \frac{R(\gamma_{SV} - \gamma_{SL})}{4\eta z} \quad (2)$$

is proportional to the cross-sectional dimension of the capillary as well as inversely proportional to the length of capillary that contains the liquid and to the viscosity of the liquid. The rate of filling decreases as the capillary fills or when a more viscous liquid is used.

The shape of the imbibition front strongly depends on the interfacial free energies. Kim et al. characterized the system and studied this relationship qualitatively using gold surfaces derivatized by SAMs of alkanethiolates terminated in different head groups (Figure 26).[189] In agreement with Equation (2), the product of the length of filling and the rate of filling $[z(dz/dt)]$ shows a linear dependence on the cosine of the advancing contact angles θ_a. The SEM images of the fronts (insets in Figure 26) indicate that different values of $\cos\theta_a$ result in different shapes of imbibing liquids: 1) For liquids with small advancing contact angles (Figure 26a, b) the imbibition fronts can be characterized as slipping films; 2) for liquids with intermediate advancing contact angles (Figure 26c, d) the shapes of the imbibition fronts consist of leading edges that suggest slipping films with shoulders; 3) for

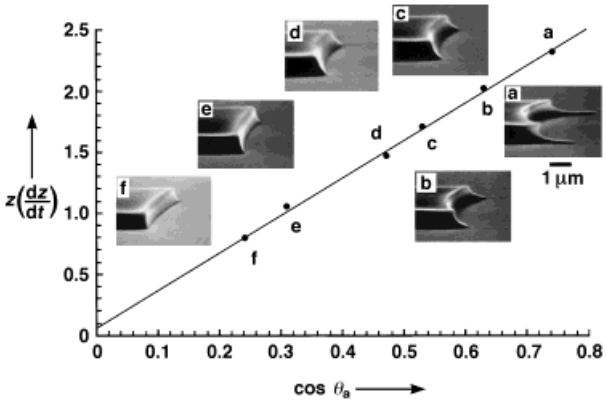

Figure 26. Dependence of the rate of capillary filling, represented by $z(dz/dt)$ in $10^4\ \mu m^2 s^{-1}$, and the imbibition shape (insets) on interfacial free energies of the surfaces[189] as described with the the dynamic contact angle θ_a between the liquid polymer and the SAM-derivatized surface.

liquids with high advancing contact angles (Figure 26e, f) the bulk liquids flow as a whole without having precursor structures. The imbibition shapes can be described as wedge or bulk-flow.

4.3.2. MIMIC of Solventless Systems

The capability and feasibility of MIMIC have been demonstrated by the fabrication of patterned structures from a variety of liquid prepolymers: PU, polyacrylates, and epoxies.[37, 179] These prepolymers have a shrinkage of less than 3% after curing.[171] The cured polymers, therefore, possess almost the exact dimensions and shapes of the channels in the surface of the PDMS mold; they can be directly used as masks in the etching of the underlying substrates. Figure 27 shows SEM images of polymeric microstructures that were fabricated by MIMIC. The polymer

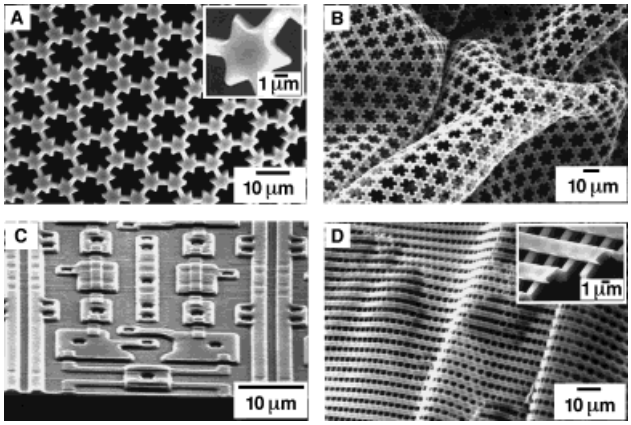

Figure 27. SEM images of polymeric microstructures fabricated by MIMIC from prepolymer of polyacrylate (A, C) and polyurethane (B, D) without solvents.[37, 179] The structures in B and D are freestanding; the buckling occurred during sample preparation and demonstrated their strength.

microstructure could be freed from the support by dissolving a sacrificial layer of glass or SiO_2 in an aqueous solution of HF/NH_4F (Figure 27B).[37] MIMIC also allows quasi-three-dimensional processing (i.e., patterning layers with different thicknesses) in a single step (Figure 27C).[179] Such complex arrays of micro and submicrometer scale channels filled completely; in some regions of these structures, features are connected to one another by channels with thicknesses of less than 100 nm. The support used in MIMIC could have relief patterns on its own surface. Figure 27D shows the SEM image of a free-standing microstructure of PU that was formed between two PDMS molds.[37, 179] Each PDMS mold has a relief pattern of parallel lines on its own surface. After the filling with liquid prepolymer and the curing of the prepolymer into a solid, the two PDMS molds were separated. The cross-linked polymeric microstructure remained on the surface of one of the two PDMS molds and could be easily released. These two layers of polymeric lines formed *one* interconnected polymeric microstructure. This type of free-standing microstructure, two layers with an independent relief structure in each, cannot be fabricated by photolithography.[10]

4.3.3. MIMIC of Systems with Solvents

Although MIMIC was developed based on prepolymers having no solvents, it has also been extended to those systems where solvents are involved.[182–186] The solvents were evaporated after the solutions had filled the channels. The only requirement seems to be that the solvent does not swell PDMS. It has been extremely difficult (or impossible) to fabricate patterned structures of those materials such as polymer beads (Figure 28A, B) and ceramics (Figure 28E, F)

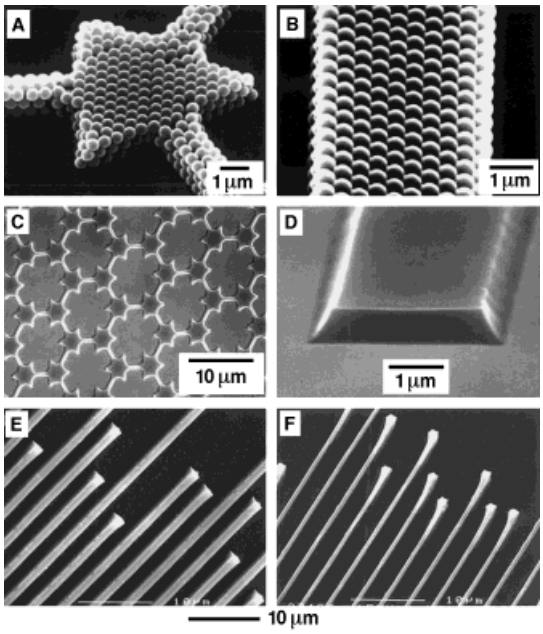

Figure 28. SEM images of patterned microstructures of A, B) polymer beads,[183] C, D) polyaniline emeraldine HCl salt,[182] and E, F) zirconium oxide[180] fabricated by MIMIC from their solutions in water, *N*-methyl-2-pyrrolidone, and ethanol, respectively. The crystallization of the polymer beads occured spontaneously. The structures of polyaniline were molded from a solution of polyaniline emeraldine base in *N*-methyl-2-pyrrolidone, and then converted into the conductive form of emeraldine salt by doping in aqueous HCl. The zirconium oxide was formed from a precursor polymer that has been molded into the structure shown in E. The precursor polymer was obtained from Chemat Technology (ZO9303), and was converted into ZrO_2 by heating at about 600 °C for 10 h. The ends of the lines deadhered from the substrate during thermal conversion.

with photolithography. Figure 28 shows SEM images of some patterned microstructures that were fabricated by MIMIC from systems involving solvents or suspending liquids. The ability to form patterned microstructures offers new opportunities for these materials. For example, the closely packed, multilayered structures of polymer beads are interesting for potential applications in chromatography and diffractive optics.[192] The ability to form patterned microstructures of conducting polymers provides a potential route to flexible, all-plastic electronic and optoelectronic devices.[193]

4.3.4. Fabrication of Functional Microelectronic Devices

Nuzzo et al. fabricated ferroelectric capacitors made up of thin films of Pt/Pb(Zr,Ti)O_3/Pt by μCP and selective CVD.[194] Recently Hu, Jeon et al. used MIMIC successfully to fabricate simple, electrically functional devices.[195–197] They demonstrated the fabrication of Schottky diodes,[195] GaAs/AlGaAs heterostructure field effect transistors (FETs),[196] and silicon metal oxide semiconductor FETs (MOSFETs).[197] The fabrication process for both types of transistors required at least three MIMIC steps and two registration steps. Figure 29 outlines the fabrication of the GaAs/AlGaAs heterostructure FET.[196] Figure 30 A shows the oblique view of the device. The source and drain are AuNiGe ohmic contacts, the channel is defined by a mesa etch, and the gate is a Cr/Au Schottky contact. In each step the pattern was defined by microstructures of PU formed by MIMIC (see Figure 29): Etching and evaporation were performed using these PU structures as the masks. Figure 30 B shows an optical micrograph of the FET, and Figure 30 C the performance of a representative GaAs/AlGaAs FET fabricated by this procedure. Its characteristics are similar to those of GaAs/AlGaAs FETs made using conventional photolithographic techniques as the patterning tools. The fabrication of the Si MOSFETs followed a similar procedure, but used PU microstructures to form the mask layers used during implantation of the silicon.[197] Although the feature sizes (16–26 μm) that characterize these devices are about 100 larger than those of state-of-the-art commercial devices (ca. 250 nm), these results established that soft lithography is compatible with the multilayer fabrication that has, up to now, been monopolized by photolithography and set a benchmark against which to measure further developments in this area.

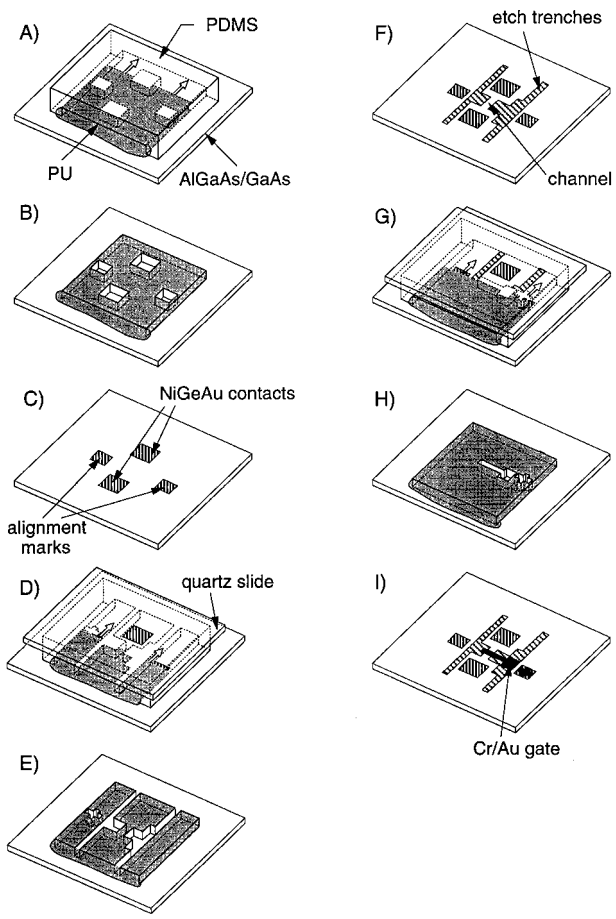

Figure 29. Schematic illustration of the procedure for the fabrication of GaAs/AlGaAs FETs.[196] A) Use MIMIC to define ohmic contacts and alignment marks. B) Cure PU, peel off the PDMS mold, and remove the thin film of PU adjoining the microstructures. C) Evaporate AuNiGe, lift off PU, anneal to form ohmic contacts for the source, and drain. D) Register and use MIMIC with another PDMS mold to define etch trenches. E) Cure PU, peel off the PDMS mold, and remove the connecting film of PU. F) Etch in an aqueous solution of citric acid and hydrogen peroxide to remove the 2DEG in the etched trenches. G) Register and use MIMIC with a third PDMS mold to define the gate. H) Cure PU, peel off the PDMS mold, and remove the thin film of PU. I) Evaporate Cr/Au and lift off PU to form the gate.

4.4. Solvent-Assisted Micromolding

Solvent-assisted micromolding (SAMIM) is a technique that allows fabrication of patterned, quasi-three-dimensional microstructures on the surfaces of polymeric substrates.[38] It can also be used to modify surface morphologies of polymers. The operational principle of this technique shares characteristics with both replica molding and embossing (see Figure 17 D). An elastomeric PDMS mold is wetted with a solvent that is a good solvent for the polymer, and is brought into contact with the surface of the polymer. The solvent dissolves (or swells) a thin layer of the polymer, and the resulting (probably gellike) fluid comprising polymer and solvent conforms to the surface topology of the mold. While the mold is maintained in conformal contact with the substrate, the polymer solidifies as the solvent dissipates and evaporates (probably by diffusion through the mold) to form relief structures with a pattern complementary to that on the surface of the mold.

SAMIM is an experimentally simple procedure. The key elements are wetting of the PDMS mold by a liquid that is a solvent for the polymer to be molded and conformal contact between the solvent-coated elastomeric mold and the substrate. The choice of solvent for a polymer determines the effectiveness and success of SAMIM. The solvent should rapidly dissolve or swell the surface of the polymer; it should not, however, swell the PDMS mold and thereby distort the mold and/or destroy the conformal contact between the polymer and the mold.[126] In general, the solvent should have a relatively high vapor pressure and a moderately high surface tension (e.g., methanol, ethanol, and acetone) to ensure rapid

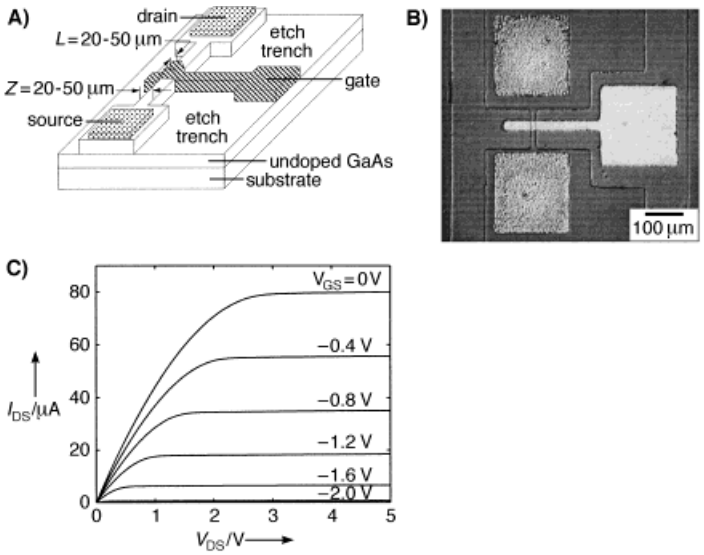

Figure 30. A) Schematic diagram of a GaAs/AlGaAs FET. B) Optical micrograph of a GaAs/AlGaAs FET fabricated by MIMIC (gate length $L = 26$ μm, gate width $Z = 16$ μm).[196] C) The performance of a representative GaAs/AlGaAs FET fabricated by this procedure.[196] I_{DS} = current between drain and source, V_{DS} = voltage between drain and source, V_{GS} = voltage between gate and source.

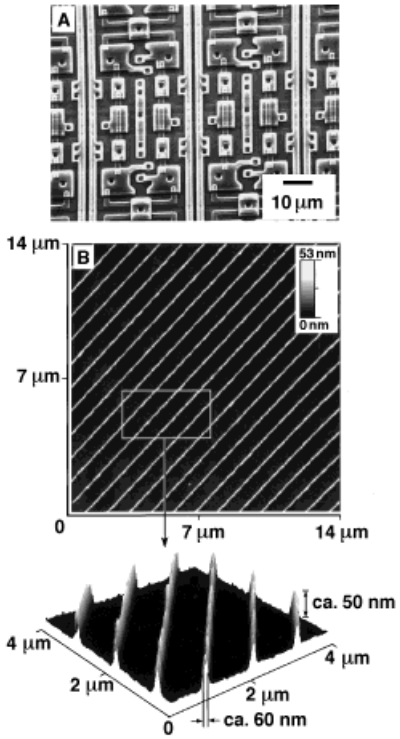

Figure 31. A) SEM and B) AFM images of polymeric microstructures fabricated by SAMIM.[38] The polymers used here were thin films (A: ca. 1.6 μm thick; B: ca. 0.4 μm thick) of a photoresist (Microposit 1805, Shipley) that was spin-coated on Si wafers. The solvent was ethanol.

evaporation of the excess solvent and minimal swelling of the PDMS mold. Dyes and inorganic salts can also be added to the solvent; they are subsequently incorporated into the resulting microstructures. Solvents with low vapor pressures (e.g., ethylene glycol and dimethyl sulfoxide) are not well suited for SAMIM. Surface modification[122] of the PDMS mold may be required when solvents with high surface tensions are used since they only partially wet the PDMS surface. Many nonpolar solvents (e.g., toluene and dichloromethane) cannot be used in SAMIM because they can swell the PDMS mold.

Replication of patterns with complex topology is practical in a single step by SAMIM. This procedure is also suitable for forming patterned relief microstructures over a large area and is applicable to a variety of polymers when appropriate solvents are selected, for example, ethanol or 2-propanol for Microposit photoresists (a phenol formadehyde resin) or acetone for polystyrene, poly(methyl methacrylate), cellulose acetate, and poly(acrylonitrile-butadiene-styrene). Figure 31 A shows the SEM image of patterned relief structures formed on a polystyrene film with acetone as the solvent.[38] These quasi-three-dimensional features are well defined and clearly resolved. A common characteristic of patterned microstructures generated by SAMIM is that the resulting structures are adjoined by a thin film of the polymer. These films can sometimes be removed by homogeneous thinning by reactive-ion etching with O_2. Figure 31 B shows AFM images of the smallest features that we have generated in a thin film of photoresist by SAMIM with ethanol as the solvent: parallel lines that are about 60 nm in width and about 50 nm in height.[38]

SAMIM can generate quasi-three-dimensional microstructures or morphologies on the surface of a polymer using a solvent that can soften the polymer without affecting the PDMS mold. SAMIM differs from other existing techniques (e.g., embossing with a rigid master[18] or MIMIC) in several ways. First, it uses an elastomeric rather than a rigid mold. Second, it uses a solvent instead of increased temperatures to "soften" the surface of the polymer. The process is simple, rapid, and does not require specialized equipment or a system for pressing the mold into the substrate. Third, it does not suffer from slow rates of capillary filling, which limits MIMIC to relatively small areas; it is also not restricted to fabrication of hydraulically connected structures. Fourth, it can be used with a wide range of polymers or prepolymers: the only requirement seems to be a solvent that dissolves the polymer of the substrate and wets the surface of the PDMS mold but does not significantly swell the mold.

5. Summary and Outlook

As fabrication of microstructures grows in importance in a wide range of areas—from microelectronics through optics, microanalysis, combinatorial synthesis, display, and MEMS to cell biology—the utility of new methods for patterning will certainly increase. The techniques of soft lithography—self-assembly, contact printing, micromolding, and contact phase-shift photolithography[115]—illustrate the potential for application of the largely unexplored, non-photolithographic procedures for micro- and nanofabrication to these new areas.

Soft lithography offers immediate advantages (Table 8) in applications in which photolithography clearly falters or fails: For example, manufacturing below the scale of 100 nm, patterning on nonplanar surfaces, fabrication of three-dimensional structures, patterning of functional materials other than

Table 8. Advantages and disadvantages of soft lithography.

Advantages
- convenient, inexpensive, accessible to chemists, biologists, and material scientists
- basis in self-assembly tends to minimize certain types of defects
- many soft lithographic processes are additive and minimize waste of materials
- readily adapted to rapid prototyping for feature sizes $>20\ \mu m$
- isotropic mechanical deformation of PDMS mold or stamp provides routes to complex patterns
- no diffraction limit; features as small as 30 nm have been fabricated
- nonplanar surfaces (lenses, optical fibers, and capillaries) can be used as substrates
- generation and replication of three-dimensional topologies or structures are possible
- optical transparency of the mask allows through-mask registration and processing
- good control over surface chemistry, very useful for interfacial engineering
- a broad range of materials can be used: functional polymers, sol–gel materials, colloidal materials, suspensions, solutions of salts, and precursors to carbon materials, glasses, and ceramics
- applicable to manufacturing: production of indistinguishable copies at low cost
- applicable in patterning large areas

Disadvantages and Problems
- patterns in the stamp or mold may distort due to the deformation (pairing, sagging, swelling, and shrinking) of the elastomer used
- difficulty in achieving accurate registration with elastomers ($<1\ \mu m$)
- compatibility with current itegrate-circuit processes and materials must be demonstrated
- defect levels higher than for photolithography
- μCP works well with only a limited range of surfaces; MIMIC is slow; REM, μTM, and SAMIM leave a thin film of polymer over the surface

photoresists, and modification of surfaces. Figure 32 summarizes the current state of development of soft lithography as well areas in which its potential is particularly clear. Most work in soft lithography has concentrated on single-step processing; our recent successes in multilayer fabrication requiring registration (albeit with features of about 20 μm) has established a modest potential in multilayer structures and functional microelectronic devices.[194–197] This demonstration paves the way for the evaluation of soft lithographic techniques in microelectronics, although serious technological use will require substantial further development.

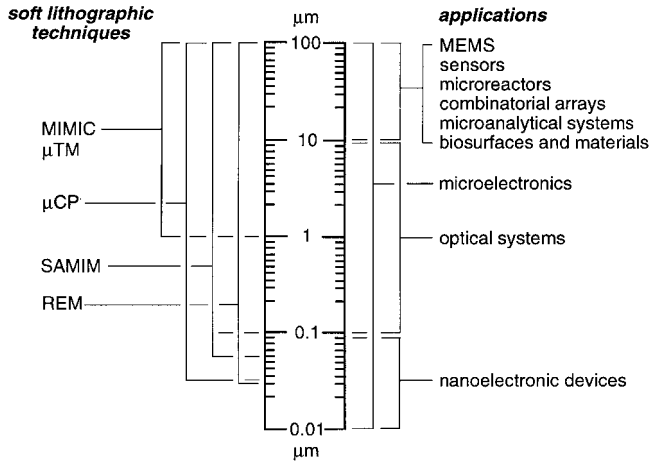

Figure 32. Summary of the current state of development of soft lithographic techniques and areas in which these techniques find applications.

Photolithography will of course continue as the dominant technology in microfabrication of technologically sophisticated semiconductor devices and systems for the foreseeable future. There are, however, many existing and emerging uses for soft lithography that take advantage of (or require) the characteristics of these techniques. Soft lithographic materials offer experimental simplicity and flexibility in forming certain types of patterns. Procedures involving relatively large features ($>1\ \mu m$) can be conducted in an unprotected laboratory environment, and thus are especially useful in laboratories that do not have routine access to the facilities normally used in microfabrication, or for which the capital cost of equipment is a serious concern. At the current state of development, they can replace photolithographic techniques in many problems of microfabrication where requirements for precise alignment, continuity, isolation, and uniformity in the final patterns are relaxed: for example, production of single-level structures for use in microelectrode arrays, sensors, biosensors, and microanalytical systems. Simple display devices, optical components, and elementary microelectronic devices also now seem practical. The initial success of soft lithography also suggests that it will be useful to reexamine other relatively undeveloped patterning techniques (see Table 2) for their potential for application in emerging technologies or in high-resolution patterning.

A number of issues remain to be solved before soft lithography invades the core applications of photolithography, that is, those in microelectronics. First, high-resolution (≤ 20 nm) registration with elastomeric materials must be demonstrated. The distortion and deformation associated with elastomeric materials must also be managed, and pattern transfer must be made exactly reproducible. Second, the quality of the patterns and structures produced must be improved. These patterns, especially for narrow lines, are not yet compatible with the levels of quality required for microfabrication of complex electronic devices. The formation and distribution of defects in SAMs, and especially their influence on the quality of patterns formed when they are used as resists for etching, must be understood and improved. Third, the compatibility of these patterning techniques with the range of processes used in the production of microelectronic circuitry must be explored. In particular, systems that form SAMs directly on semiconductors and are optimized for compatibility with current processes (especially etching with reactive ions) and materials are required.

Researchers and manufacturers of microstructures have specific requirements of any microlithographic technology: flexibility during the development process; reproducibility, reliability, and simplicity during manufacturing; and cost-effectiveness for commercial success. Judged against these standards, soft lithography has the potential to become an important addition to the field of micro- and nanofabrication, although it is still in an early stage of technical development.

This work was supported in part by the Office of Naval Research (ONR) and the Defense Advanced Research Projects Agency (DARPA). This work made use of Material Research Science and Engineering Center (MRSEC) Shared Facilities supported by the National Science Foundation (NSF) under

award number DMR-9400396. We thank our colleagues and collaborators for their essential contributions to this work: Colin Bain, Paul Laibinis, John Folkers, Hans Biebuyck, Ralph Nuzzo, Mark Wrighton, and Mara Prentiss (SAMs); Amit Kumar, Hans Biebuyck, Nicholas Abbott, James Wilbur, John Rogers, Rebecca Jackman, Gabriel López, and Ralph Nuzzo (μCP); Enoch Kim, Xiao-Mei Zhao (molding and related techniques); Dong Qin (rapid prototyping); John Rogers, Kateri Paul, and Joanna Aizenberg (contact phase shift photolithography); and Junmin Hu, Noo-Li Jeon, Ralph Nuzzo, and Robert Westervelt (fabrication of microelectronic devices). We also thank Dr. Hans Biebuyck for providing the STM images shown in Figure 9, and the IBM Zurich group for providing data before publication.

Received: July 4, 1997 [A239IE]
German version: *Angew. Chem.* **1998**, *110*, 568 – 594

[1] General reviews on nanoscience and nanotechnology: a) *Science* **1991**, *254*, 1300 – 1342; b) G. A. Ozin, *Adv. Mater.* **1991**, *4*, 612 – 649; c) G. Stix, *Sci. Am.* **1995**, *272*(2), 90 – 96.

[2] General accounts on the development of microelectronics: a) R. W. Keyes, *Phys. Today* **1992**, *45*(8), 42 – 48; b) C. R. Barrett, *MRS Bull.* **1993**, *28*(7), 3 – 10; c) R. F. Service, *Science* **1996**, *273*, 1834 – 1836; d) G. Moore, *Electrochem. Soc. Interf.* **1997**, 18 – 23.

[3] General reviews on QSE: a) M. Sundaram, S. A. Chalmers, P. F. Hopkins, A. C. Gossard, *Science* **1991**, *254*, 1326 – 1335; b) M. A. Kastner, *Phys. Today* **1993**, *46*(1), 24 – 31; c) M. A. Reed, *Sci. Am.* **1993**, *270*(1), 118 – 123; d) H. Weller, *Angew. Chem.* **1993**, *105*, 43 – 56; *Angew. Chem. Int. Ed. Engl.* **1993**, *32*, 41 – 53.

[4] General reviews on SET: a) K. K. Likharev, *IBM J. Res. Dev.* **1988**, *32*, 144 – 158; b) M. H. Devoret, D. Esteve, C. Urbina, *Nature* **1992**, *360*, 547 – 553; c) K. K. Likharev, T. Claeson, *Sci. Am.* **1992**, *269*(6), 80 – 85.

[5] General reviews on microelectromechanical systems (MEMS): a) K. D. Wise, K. Najafi, *Science* **1991**, *254*, 1335 – 1342; b) J. Bryzek, K. Peterson, W. McCulley, *IEEE Spectrum* **1994**, *31*(5), 20 – 31; c) N. C. MacDonald, *Microelectron. Eng.* **1996**, *32*, 49 – 73; d) G. T. A. Kovacs, K. Petersen, M. Albin, *Anal. Chem.* **1996**, *68*, 407A – 412A.

[6] General reviews and highlights on microanalytical systems: a) R. E. Service, *Science* **1995**, *268*, 26 – 27; b) A. Manz, *Chimia* **1996**, *59*, 140 – 145; c) D. Craston, S. Cowen, *Chem. Br.* **1996**(10), 31 – 33; d) P. Day, *ibid.* **1996**(7), 29 – 31; e) A. Goffeau, *Nature* **1997**, *385*, 202 – 203.

[7] Recent reports on microoptics: a) Y. A. Carts, *Laser Focus World* **1994**, *30*, 67 – 71; b) S. S. Lee, L. Y. Lin, M. C. Wu, *Appl. Phys. Lett.* **1995**, *67*, 2135 – 2137; c) M. C. Wu, L. Y. Lin, S. S. Lee, C. R. King, *Laser Focus World* **1996**, *32*, 64 – 68.

[8] General reviews on microsensors: a) H.-J. Galla, *Angew. Chem.* **1992**, *104*, 47 – 50; *Angew. Chem. Int. Ed. Engl.* **1992**, *31*, 45 – 47; b) P. Kleinschmidt, W. Hanrieder, *Sens. Actuators A* **1992**, *33*, 5 – 17; c) M. J. Vellekoop, G. W. Lubking, P. M. Sarro, A. Venema, *ibid.* **1994**, *44*, 249 – 263; d) G. Fuhr, T. Müller, T. Schnelle, R. Hagedorn, A. Voigt, S. Fiedler, W. A. Arnold, U. Zimmermann, B. Wagner, A. Heuberger, *Naturwissenschaften* **1994**, *81*, 528 – 535; e) J. Bryzek, *Sensors* **1996,** 7, 4 – 38.

[9] Recent reviews on combinatorial synthesis: *Chem. Rev.* **1997**, *97*, 347 – 509.

[10] General reviews on photolithography: a) S. Okazaki, *J. Vac. Sci. Technol. B* **1991**, *9*, 2829 – 2833; b) H. J. Jeong, D. A. Markle, G. Owen, F. Pease, A. Grenville, R. von Bünau, *Solid State Technol.* **1994**, *37*, 39 – 47; c) M. D. Levenson, *ibid.* **1995**, *38*, 57 – 66; d) L. Geppert, *IEEE Spectrum* **1996**, *33*(4), 33 – 38.

[11] General reviews on microlithographic techniques: a) W. M. Moreau, *Semiconductor Lithography: Principles and Materials*, Plenum, New York, **1988**; b) D. Brambley, B. Martin, P. D. Prewett, *Adv. Mater. Opt. Electron.* **1994**, *4*, 55 – 74; c) *Handbook of Microlithography, Micromachining, and Microfabrication, Vol. 1* (Ed.: P. Rai-Choudhury), SPIE Optical Engineering Press, Bellingham, WA, **1997**.

[12] General reviews on nanolithography: a) R. F. W. Pease, *J. Vac. Sci. Technol. B* **1992**, *10*, 278 – 285; b) F. Cerrina, C. Marrian, *MRS Bull.* **1996**, *31*(12), 56 – 62; c) *Microelectron. Eng.* **1996**, *32*, 1 – 418.

[13] See, for example, a) W. D. Deninger, C. E. Garner, *J. Vac. Sci. Technol. B* **1988**, *6*, 337 – 340; b) R. G. Vadimsky, *ibid.* **1988**, *6*, 2221 – 2223.

[14] General reviews on photoresists: a) E. Reichmanis, L. F. Thompson, *Chem. Rev.* **1989**, *89*, 1273 – 1289; b) R. D. Miller, G. M. Wallraff, *Adv. Mater. Opt. E1ectron.* **1994**, *4*, 95 – 127; c) A. Reiser, H.-Y. Shih, T.-F. Yeh, J.-P. Huang, *Angew. Chem.* **1996**, *108*, 2609 – 2620; *Angew. Chem. Int. Ed. Engl.* **1996**, *35*, 2428 – 2440.

[15] Injection molding on the micrometer scale: a) P. E. J. Legierse, J. H. T. Pasman in *Polymers in Information Storage Technology*, Plenum, New York, **1989**, p. 155; b) W. Michaeli, R. Bielzer, *Adv. Mater.* **1991**, *3*, 260 – 262; c) T. E. Huber, L. Luo, *Appl. Phys. Lett.* **1997**, *70*, 2502 – 2504.

[16] Injection molding on the nanometer scale: a) P. Hoyer, N. Baba, H. Masuda, *Appl. Phys. Lett.* **1995**, *66*, 2700 – 2702; b) H. Masuda, K. Fukuda, *Science* **1995**, *268*, 1466 – 1468; c) P. Hoyer, *Adv. Mater.* **1996**, *8*, 857 – 859.

[17] Embossing on the micrometer scale: a) J. S. Winslow, *IEEE Trans. Consumer Electron.* **1976** (Nov.), 318 – 326; b) H. W. Lehmann, R. Widmer, M. Ebnoether, A. Wokaun, M. Meier, S. K. Miller, *J. Vac. Sci. Technol. B* **1983**, *1*, 1207 – 1210; c) C. M. Rodia, *Proc. SPIE Int. Soc. Opt. Eng.* **1985**, *529*, 69 – 75; d) K.-H. Schlereth, H. Bötther, *J. Vac. Sci. Technol. B* **1992**, *10*, 114 – 117; e) M. Emmelius, G. Pawlowski, H. W. Vollmann, *Angew. Chem.* **1989**, *101*, 1475 – 1501; *Angew. Chem. Int. Ed. Engl.* **1989**, *28*, 1445 – 1471; f) F. P. Shvartsman in *Diffractive and Miniaturized Optics* (Ed.: S.-H. Lee), SPIE Optical Engineering Press, Bellingham, WA, **1993**, pp. 165 – 186.

[18] Embossing on the nanometer scale: a) S. Y. Chou, P. R. Krauss, P. J. Renstrom, *Appl. Phys. Lett.* **1995**, *67*, 3114 – 3116; b) *Science* **1996**, *272*, 85 – 87; c) M. T. Gale in *Micro-Optics: Elements, Systems and Applications* (Ed.: H. P. Herzig), Taylor & Francis, London, **1997**, pp. 153 – 179.

[19] Cast molding on the micrometer scale: a) H. C. Haverkorn van Rijsewijk, P. E. J. Legierse, G. E. Thomas, *Philips Tech. Rev.* **1982**, *40*, 287 – 297; b) J. G. Kloosterboer, G. J. M. Lippits, H. C. Meinders, *ibid.* **1982**, *40*, 198 – 309.

[20] Cast molding on the nanometer scale: B. D. Terris, H. J. Mamin, M. E. Best, J. A. Logan, D. Rugar, *Appl. Phys. Lett.* **1996**, *69*, 4262 – 4264.

[21] Laser ablation on the micrometer scale: a) U. Reblan, H. Endert, G. Zaal, *Laser Focus World* **1994**, *30*, 91 – 96; b) S. A. Weiss, *Photonics Spectra* **1995**, *29*(10), 108 – 114; c) M. A. Roberts, J. S. Rossier, P. Bercier, H. Giault, *Anal. Chem.* **1997**, *69*, 2035 – 2042.

[22] Laser ablation on the nanometer scale: a) D. Y. Kim, S. K. Tripathy, L. Li, J. Kumar, *Appl. Phys. Lett.* **1995**, *66*, 1166 – 1168; b) M. Müllenborn, H. Dirac, J. W. Peterson, *ibid.* **1995**, *66*, 3001 – 3003; c) N. Kramer, M. Niesten, C. Schönenberger, *ibid.* **1995**, *67*, 2989 – 2991.

[23] N. L. Abbott, A. Kumar, G. M. Whitesides, *Chem. Mater.* **1994**, *6*, 596 – 602.

[24] a) T. J. Hirsch, R. F. Miracky, C. Lin, *Appl. Phys. Lett.* **1990**, *57*, 1357 – 1359; b) V. Malba, A. F. Bernhardt, *ibid.* **1992**, *60*, 909 – 911; c) A. Miehr, R. A. Fisher, O. Lehmann, M. Stuke, *Adv. Mater. Opt. Electron.* **1996**, *6*, 27 – 32.

[25] M. Datta, *J. Electrochem. Soc.* **1995**, *142*, 3801 – 3806.

[26] a) H. Tabei, S. Nara, K. Matsuyama, *J. Electrochem. Soc.* **1974**, *121*, 67 – 69; b) A. Rose, P. K. Weimer, *Phys. Today* **1989**, *42*(9), 24 – 32; c) M. R. V. Sahyun, *CHEMTECH* **1992**, *22*(7), 418 – 424.

[27] S. Leppävuori, J. Väänänen, M. Lothi, J. Remes, A. Uusimäki, *Sens. Actuators A* **1994**, *41/42*, 593 – 596.

[28] H. Moilanen, J. Lappalainen, S. Leppävuori, *Sens. Actuators A* **1994**, *43*, 357 – 365.

[29] General reviews and highlights on ink-jet printing: a) M. Döring, *Philips Tech. Rev.* **1982**, *40*, 192 – 198; b) E. Anczurowski, J. Oliver, R. H. Marchessault, *CHEMTECH* **1986**, *16*(5), 304 – 310; c) C. Wu, *Sci. News* **1997**, *151*, 205.

[30] Application of ink-jet printing in combinatorial systhesis: a) A. P. Blanchard, R. J. Kaiser, L. E. Hood, *Biosens. Bioelectron.* **1996**, *11*,

687 – 690; b) A. V. Lemmo, J. T. Fisher, H. M. Geysen, D. J. Rose, *Anal. Chem.* **1997**, *69*, 543 – 551.
[31] a) M. Stolka, *CHEMTECH* **1989**, *19*(8), 487 – 495; b) Q. M. Pai, B. E. Springett, *Rev. Mod. Phys.* **1993**, *65*, 163 – 211.
[32] a) D. C. Neckers, *CHEMTECH* **1990**, *20*(10), 616 – 619; b) T. M. Bloomstein, D. J. Ehrlich, *Appl. Phys. Lett.* **1992**, *61*, 708 – 781; c) F. T. Wallenberger, *Science* **1995**, *267*, 1274 – 1275; d) O. Lehmann, M. Stuke, *ibid.* **1995**, *270*, 1644 – 1646.
[33] Short reviews on soft lithography: a) Y. Xia, Dissertation, Harvard University, USA, **1996**; b) X.-M. Zhao, Y. Xia, G. M. Whitesides, *J. Mater. Chem.* **1997**, *7*, 1069 – 1074; c) D. Qin, Y. Xia, J. A. Rogers, R. J. Jackman, X.-M. Zhao, G. M. Whitesides, *Top. Curr. Chem.* **1998**, *194*, 1 – 20; d) G. M. Whitesides, Y. Xia, *Annu. Rev. Mater. Sci.* **1998**, *28*, 153 – 184.
[34] A. Kumar, G. M. Whitesides, *Appl. Phys. Lett.* **1993**, *63*, 2002 – 2004.
[35] Y. Xia, E. Kim, X.-M. Zhao, J. A. Rogers, M. Prentiss, G. M. Whitesides, *Science* **1996**, *273*, 347 – 349.
[36] X.-M. Zhao, Y. Xia, G. M. Whitesides, *Adv. Mater.* **1996**, *8*, 837 – 840.
[37] E. Kim, Y. Xia, G. M. Whitesides, *Nature* **1995**, *376*, 581 – 584.
[38] E. Kim, Y. Xia, X.-M. Zhao, G. M. Whitesides, *Adv. Mater.* **1997**, *9*, 651 – 654.
[39] General reviews on SAMs: a) C. D. Bain, G. M. Whitesides, *Angew. Chem.* **1989**, *101*, 522 – 528; *Angew. Chem. Int. Ed. Engl.* **1989**, *28*, 506 – 512; b) G. M. Whitesides, P. E. Laibinis, *Langmuir* **1990**, *6*, 87 – 96; c) A. Ulman, *Introduction to Thin Organic Films: From Langmuir – Blodgett to Self-Assembly*, Academic Press, Boston, **1991**; d) J. D. Swalen, *Annu. Rev. Mater. Sci.* **1991**, *21*, 373 – 408; e) L. H. Dubois, R. G. Nuzzo, *Annu. Rev. Phys. Chem.* **1992**, *43*, 437 – 463.
[40] General reviews on self-assembly: a) J.-M. Lehn, *Angew. Chem.* **1990**, *102*, 1347 – 1362; *Angew. Chem. Int. Ed. Engl.* **1990**, *29*, 1304 – 1319; b) G. M. Whitesides, J. P. Mathias, C. T. Seto, *Science* **1991**, *254*, 1312 – 1319; c) G. M. Whitesides, *Sci. Am.* **1995**, *273*(9), 146 – 149.
[41] a) T. E. Creigton, *Proteins: Structures and Molecular Properties*, Freeman, New York, **1983**; b) W. Sanger, *Principles of Nucleic Acid Structures*, Springer, New York, **1986**; c) H. Ringsdorf, B. Schlarb, J. Venzmer, *Angew. Chem.* **1988**, *100*, 117 – 162; *Angew. Chem. Int. Ed. Engl.* **1988**, *27*, 113 – 158.
[42] Self-assembly on the molecular scale: a) J.-M. Lehn, *Angew. Chem.* **1988**, *100*, 91 – 114; *Angew. Chem. Int. Ed. Engl.* **1988**, *27*, 89 – 112; b) J. S. Lindsey, *New J. Chem.* **1991**, *15*, 153 – 180; c) E. E. Simanek, J. P. Mathias, C. T. Seto, D. Chin, M. Mammen, D. M. Gordon, G. M. Whitesides, *Acc. Chem. Res.* **1995**, *28*, 37 – 44; d) V. Percec, J. Heck, G. Johansson, D. Tornazos, M. Kawosumi, *Pure Appl. Chem.* **1994**, *A31*, 1031 – 1070.
[43] Self-assembly on the nanometer scale: a) C. A. Mirkin, R. L. Letsinger, R. C. Mucic, J. J. Storhuff, *Nature* **1996**, *382*, 607 – 609; b) A. P. Alivisator, K. P. Johnsson, X. Peng, T. E. Wilson, C. J. Loweth, M. P. Bruchez, Jr., P. G. Schurtz, *Nature* **1996**, *382*, 609 – 611.
[44] Self-assembly on the micrometer scale: a) A. S. Dimitov, K. Nagayama, *Langmuir* **1996**, *12*, 1303 – 1311; b) M. Trau, S. Sankaran, D. A. Saville, I. A. Aksay, *Nature* **1995**, *374*, 437 – 439; c) S.-R. Yeh, M. Seul, B. I. Shraiman, *ibid.* **1997**, *386*, 57 – 59; d) A. van Blaaderen, R. Ruel, P. Wiltzius, *ibid.* **1997**, *385*, 321 – 324.
[45] Self-assembly on the millimeter scale: a) A. Terfort, N. Bowden, G. M. Whitesides, *Nature* **1997**, *386*, 162 – 164; b) N. Bowden, A. Terfort, J. Carbeck, G. M. Whitesides, *Science* **1997**, *276*, 233 – 235.
[46] Recent reviews on SAMs: a) J. Xu, H.-L. Li, *J. Coll. Interf. Sci.* **1995**, *176*, 138 – 149; b) A. Ulman, *MRS Bull.* **1995**, *30*(6), 46 – 51; c) A. R. Bishop, R. G. Nuzzo, *Curr. Opin. Coll. Interf. Sci.* **1996**, *1*, 127 – 136; d) E. Delamarche, B. Michel, H. A. Biebuyck, C. Gerber, *Adv. Mater.* **1996**, *8*, 719 – 729.
[47] See, for example, a) P. Fenter, A. Eberhardt, P. Eisenberger, *Science* **1994**, *266*, 1216 – 1218; b) E. Delamarche, B. Michel, H. Kang, C. Gerber, *Langmuir* **1994**, *10*, 4103 – 4108; c) S. V. Atre, B. Liedberg, D. L. Allara, *ibid.* **1995**, *11*, 3882 – 3893; d) P. Wagner, M. Hegner, H.-J. Güntherodt, G. Sernenza, *ibid.* **1995**, *11*, 3867 – 3875.
[48] See, for example, a) H. A. Biebuyck, G. M. Whitesides, *Langmuir* **1994**, *10*, 1825 – 1831; b) H. Schönherr, H. Ringsdorf, *ibid.* **1996**, *12*, 3891 – 3897.
[49] E. B. Throughton, C. D. Bain, G. M. Whitesides, R. G. Nuzzo, D. L. Allara, M. D. Porter, *Langmuir* **1988**, *4*, 365 – 385.
[50] J. E. Chadwick, D. C. Myles, R. L. Garrell, *J. Am. Chem. Soc.* **1993**, *115*, 10364 – 10365.
[51] K. Uvdal, I. Persson, B. Liedberg, *Langmuir* **1995**, *11*, 1252 – 1256.
[52] See, for example, a) P. Fenter, P. Eisenberger, J. Li, N. Camillone III, S. Bernasek, G. Scoles, T. A. Ramnanarayanan, K. S. Liang, *Langmuir* **1991**, *7*, 2013 – 2016; b) A. Dhirani, M. A. Hines, A. J. Fisher, O. Ismail, P. Guyot-Sionnest, *ibid.* **1995**, *11*, 2609 – 2614.
[53] See, for example, a) H. Keller, P. Sirnak, W. Schrepp, J. Dembowski, *Thin Solid Films* **1994**, *244*, 799 – 805; b) M. Itoh, K. Nishihara, K. Aramaki, *J. Electrochem. Soc.* **1995**, *142*, 3696 – 3704; c) J. B. Schlenoff, M. Li, H. Ly, *J. Am. Chem. Soc.* **1995**, *117*, 12528 – 12536.
[54] T. R. Lee, P. E. Laibinis, J. P. Folkers, G. M. Whitesides, *Pure Appl. Chem.* **1991**, *63*, 821 – 828.
[55] J. J. Hickman, P. E. Laibinis, D. I. Auerbach, C. Zou, T. J. Gardner, G. M. Whitesides, M. S. Wrighton, *Langmuir* **1992**, *8*, 357 – 359.
[56] See, for example, a) C. W. Sheen, J.-X. Shi, J. Martensson, A. N. Parikh, D. L. Allara, *J. Am. Chem. Soc.* **1992**, *114*, 1514 – 1515; b) C. D. Bain, *Adv. Mater.* **1992**, *4*, 591 – 594; c) J. F. Dorsten, J. E. Maslar, P. W. Bohn, *Appl. Phys. Lett.* **1995**, *66*, 1755 – 1757.
[57] Y. Gu, Z. Lin, R. A. Butera, V. S. Smentkowski, D. H. Waldeck, *Langmuir* **1995**, *11*, 1849 – 1851.
[58] See, for example, a) M. J. Wirth, R. W. P. Fairbank, H. O. Fatunmbi, *Science* **1997**, *275*, 44 – 47; b) J. B. Brzoska, I. B. Azouz, F. Rondelez, *Langmuir* **1994**, *10*, 4367 – 4373; c) D. L. Allara, A. N. Parikh, F. Rondelez, *ibid.* **1995**, *11*, 2357 – 2360.
[59] M. R. Linford, C. E. D. Chidsey, *J. Am. Chem. Soc.* **1993**, *115*, 12631 – 12632.
[60] M. R. Linford, P. Fenter, P. M. Eisenberger, C. E. D. Chidsey, *J. Am. Chem. Soc.* **1995**, *117*, 3145 – 3155.
[61] A. Bansal, X. Li, I. Lauermann, N. S. Lewis, S. I. Yi, W. H. Weinberg, *J. Am. Chem. Soc.* **1996**, *118*, 7225 – 7226.
[62] See, for example, a) D. L. Allara, R. G. Nuzzo, *Langmuir* **1985**, *1*, 54 – 71; b) P. E. Laibinis, J. J. Hickinan, M. S. Wrighton, G. M. Whitesides, *Science* **1989**, *245*, 845 – 847; c) Y.-T. Tao, M.-T. Lee, S.-C. Chang, *J. Am. Chem. Soc.* **1993**, *115*, 9547 – 9555.
[63] J. P. Folkers, C. B. Gorman, P. E. Laibinis, S. Buchholz, G. M. Whitesides, R. G. Nuzzo, *Langmuir* **1995**, *11*, 813 – 824.
[64] Reviews: a) G. Cao, H.-G. Hong, T. E. Mallouk, *Acc. Chem. Res.* **1992**, *25*, 420 – 427; b) M. E. Thompson, *Chem. Mater.* **1994**, *6*, 1168 – 1175; c) H. E. Katz, *ibid.* **1994**, *6*, 2227 – 2232.
[65] T. J. Gardner, C. D. Frisbie, M. S. Wrighton, *J. Am. Chem. Soc.* **1995**, *117*, 6927 – 6933.
[66] A recent review on STM studies: G. E. Polner, *Chem. Rev.* **1997**, *97*, 1117 – 1127.
[67] Recent AFM studies: a) C. A. Alves, E. L. Smith, M. D. Porter, *J. Am. Chem. Soc.* **1992**, *114*, 1222 – 1227; b) G.-Y. Liu, M. B. Salmeron, *Langmuir* **1994**, *10*, 367 – 370.
[68] See, for example, M. R. Anderson, M. N. Evaniak, M. Zhang, *Langmuir* **1996**, *12*, 294 – 300.
[69] See, for example, N. Camillone III, T. Y. B. Leung, P. Schwartz, P. Eisenberger, G. Scoles, *Langmuir* **1996**, *12*, 2737 – 2746.
[70] See, for example, W. B. Caldwell, D. J. Campbell, K. Chen, B. R. Herr, C. A. Mirkin, A. Malik, M. K. Durbin, P. Dutta, K. G. Huang, *J. Am. Chem. Soc.* **1995**, *117*, 6071 – 6082.
[71] See, for example, L. Strong, G. M. Whitesides, *Langmuir* **1988**, *4*, 546 – 558.
[72] M. A. Bryant, J. E. Pemberton, *J. Am. Chem. Soc.* **1991**, *113*, 3629 – 3637.
[73] See, for example, a) Q. Du, E. Freysz, Y. R. Shen, *Science* **1994**, *264*, 826 – 828; b) C. D. Bain, *J. Chem. Soc. Faraday Trans.* **1995**, *91*, 1281 – 1296.
[74] See, for example, J. P. Folkers, P. E. Laibinis, G. M. Whitesides, *Langmuir* **1992**, *8*, 1330 – 1341.
[75] L. H. Dubois, B. R. Zegarski, R. G. Nuzzo, *J. Am. Chem. Soc.* **1990**, *112*, 570 – 579.
[76] See, for example, a) Y. Li, J. Huang, R. T. McIver, Jr., J. C. Hemminger, *J. Am. Chem. Soc.* **1992**, *114*, 2428 – 2432; b) M. J. Tarlov, J. G. Newman, *Langmuir* **1992**, *8*, 1398 – 1405; c) T. D. McCarley, R. L. McCarley, *Anal. Chem.* **1997**, *69*, 130 – 136.
[77] See, for example, a) C. D. Bain, G. M. Whitesides, *J. Am. Chem. Soc.* **1988**, *110*, 3665 – 3666; b) D. J. Olbris, A. Ulman, Y. Shnidman, *J. Chem. Phys.* **1995**, *102*, 6885 – 6873.

[78] See, for example, C. D. Bain, E. B. Throughton, Y.-T. Tao, J. Evall, G. M. Whitesides, R. G. Nuzzo, *J. Am. Chem. Soc.* **1989**, *111*, 321 – 335.

[79] See, for example, a) D. A. Buttry, M. D. Ward, *Chem. Rev.* **1992**, *92*, 1355 – 1379; b) T. W. Schneider, D. A. Buttry, *J. Am. Chem. Soc.* **1993**, *115*, 12391 – 12397; c) D. S. Karpovich, G. J. Blanchard, *Langmuir* **1994**, *10*, 3315 – 3322; d) C. Fruböss, K. Doblhofer, *J. Chem. Soc. Faraday Trans.* **1995**, *91*, 1949 – 1953.

[80] M. D. Ward, D. A. Buttry, *Science* **1990**, *249*, 1000 – 1007.

[81] See, for example, a) S. Li, R. M. Crooks, *Langmuir* **1993**, *9*, 1951 – 1954; b) A. Badia, R. Back, R. B. Lennox, *Angew. Chem.* **1994**, *106*, 2429 – 2432; *Angew. Chem. Int. Ed. Engl.* **1994**, *33*, 2332 – 2335; c) F. P. Zamborini, R. M. Crooks, *Langmuir* **1997**, *13*, 122 – 126.

[82] X.-M. Zhao, J. L. Wilbur, G. M. Whitesides, *Langmuir* **1996**, *12*, 3257 – 3264.

[83] General reviews on interactions between SAMs and proteins/cells: a) M. Mrksich, G. M. Whitesides, *TIBTECH* **1995**, *13*, 228 – 235; b) *Annu. Rev. Biophys. Biomol. Struc.* **1996**, *25*, 55 – 78.

[84] Previous reviews on microcontact printers: a) J. L. Wilbur, A. Kumar, E. Kim, G. M. Whitesides, *Adv. Mater.* **1994**, *6*, 600 – 604; b) A. Kurnar, N. L. Abbott, E. Kim, H. A. Biebuyck, G. M. Whitesides, *Acc. Chem. Res.* **1995**, *28*, 219 – 226; c) G. M. Whitesides, C. B. Gorman in *Handbook of Surface Imaging and Visualization* (Ed.: A. T. Hubbard), CRC Press, Boca Raton, FL, **1995**, pp. 713 – 733; d) J. L. Wilbur, A. Kumar, H. A. Biebuyck, E. Kim, G. M. Whitesides, *Nanotechnology* **1996**, *7*, 452 – 457; e) Y. Xia, X.-M. Zhao, G. M. Whitesides, *Microelectron. Eng.* **1996**, *32*, 255 – 268; f) H. A. Biebuyck, N. B. Larsen, E. Delamarche, B. Michel, *IBM J. Res. Dev.* **1997**, *41*, 159 – 170.

[85] Microprinting of alkanethiols on gold: A. Kumar, H. Biebuyck, G. M. Whitesides, *Langmuir* **1994**, *10*, 1498 – 1511.

[86] Microprinting of alkanethiols on silver: a) Y. Xia, E. Kim, G. M. Whitesides, *J. Electrochem. Soc.* **1996**, *143*, 1070 – 1079; b) X. M. Yang, A. A. Tryk, K. Hasimoto, A. Fujishima, *Appl. Phys. Lett.* **1996**, *69*, 4020 – 4022.

[87] Microprinting of alkanethiols on copper: a) T. P. Moffat, H. Yang, *J. Electrochem. Soc.* **1995**, *142*, L220 – L222; b) Y. Xia, E. Kim, M. Mrksich, G. M. Whitesides, *Chem. Mater.* **1996**, *8*, 601 – 603.

[88] Microprinting of alkanethiols on palladium: L. Goetting, N.-L. Jeon, G. M. Whitesides, unpublished results.

[89] Microprinting of RPO_3H_2 on Al/Al_2O_3: L. Goetting, G. M. Whitesides, unpublished results.

[90] Microprinting of siloxanes on Si/SiO_2: a) Y. Xia, M. Mrksich, E. Kim, G. M. Whitesides, *J. Am. Chem. Soc.* **1995**, *117*, 9576 – 9577; b) P. M. St. John, H. G. Craighead, *Appl. Phys. Lett.* **1996**, *68*, 1022 – 1024; c) D. Wang, S. G. Thomas, K. L. Wang, Y. Xia, G. M. Whitesides, *ibid*. **1997**, *70*, 1593 – 1595.

[91] Photooxidation of alkanethiolate SAMs on gold: a) J. Huang, J. C. Hemminger, *J. Am. Chem. Soc.* **1993**, *115*, 3342 – 3343; b) M. J. Tarlov, D. R. F. Burgess, Jr., G. Gillen, *ibid*. **1993**, *115*, 5305 – 5306; c) J. Huang, D. A. Dahlgren, J. C. Hemminger, *Langmuir* **1994**, *10*, 626 – 628; d) S.-W. Tam-Chang, H. A. Biebuyck, G. M. Whitesides, N. Jeon, R. G. Nuzzo, *ibid*. **1995**, *11*, 4371 – 4382; e) D. A. Hutt, E. Cooper, L. Parker, G. J. Leggett, T. L. Parker, *ibid*. **1996**, *12*, 5494 – 5497.

[92] Photo-cross-linking of alkanethiolate SAMs on gold: a) K. C. Chan, T. Kim, J. K. Schoer, R. M. Crooks, *J. Am. Chem. Soc.* **1995**, *117*, 5875 – 5876; b) T. Kim, K. C. Chan, R. M. Crooks, *ibid*. **1997**, *119*, 189 – 193.

[93] Photoactivation of alkanethiolate SAMs on gold: a) E. W. Wollman, C. D. Frisbie, M. S. Wrighton, *Langmuir* **1993**, *9*, 1517 – 1520; b) D. J. Pritchard, H. Morgan, J. M. Cooper, *Angew. Chem.* **1995**, *107*, 84 – 86; *Angew. Chem. Int. Ed. Engl.* **1995**, *34*, 91 – 93.

[94] See, for example, A. C. Pease, D. Solas, E. J. Sullivan, M. T. Cronin, C. P. Holmes, S. P. A. Fodor, *Proc. Natl. Acad. Sci. USA* **1994**, *91*, 5022 – 5026.

[95] Recent reviews: a) W. J. Dressick, J. M. Calvert, *Jpn. J. Appl. Phys.* **1993**, *32*, 5829 – 5839; b) J. M. Calvert, *Thin Films* **1995**, *20*, 109 – 141.

[96] J. A. M. Sondag-Huethorst, H. R. J. van Helleputte, L. G. Fokkink, *Appl. Phys. Lett.* **1994**, *64*, 285 – 287.

[97] M. Lercel, R. C. Tiberio, P. F. Chapman, H. G. Craighead, C. W. Sheen, A. N. Parikh, D. L. Allara, *J. Vac. Sci. Technol. B* **1993**, *11*, 2823 – 2828.

[98] M. J. Lercel, H. G. Craighead, A. N. Parikh, K. Seshadri, A. L. Allara, *Appl. Phys. Lett.* **1996**, *68*, 1504 – 1506.

[99] G. Gillen, S. Wight, J. Bennett, M. J. Tarlov, *Appl. Phys. Lett.* **1994**, *65*, 534 – 536.

[100] a) K. K. Berggren, A. Bard, J. L. Wilbur, J. D. Gillaspy, A. G. Heig, J. J. McClelland, S. L. Rolston, W. D. Phillips, M. Prentiss, G. M. Whitesides, *Science* **1995**, *269*, 1255 – 1257; b) K. K. Berggren, R. Younkin, E. Cheung, M. Prentiss, A. J. Black, G. M. Whitesides, D. C. Ralph, O. T. Black, M. Tinkham, *Adv. Mater.* **1997**, *9*, 52 – 55.

[101] K. S. Johnson, K. K. Berggren, A. J. Black, A. P. Chu, N. H. Dekker, D. C. Ralph, J. H. Thywissen, R. Youkin, M. Prentiss, M. Tinkham, G. M. Whitesides, *Appl. Phys. Lett.* **1996**, *69*, 2773 – 2775.

[102] See, for example, a) C. B. Ross, L. Sun, R. M. Crooks, *Langmuir* **1993**, *9*, 632 – 636; b) E. Delamarche, A. C. F. Hoole, B. Michel, S. Wilkes, M. Despont, M. E. Weiland, H. Biebuyck, *J. Phys. Chem. B* **1997**, *101*, 9263 – 9269.

[103] a) N. L. Abbott, J. P. Folkers, G. M. Whitesides, *Science* **1992**, *257*, 1380 – 1382; b) N. L. Abbott, D. R. Rolison, G. M. Whitesides, *Langmuir* **1994**, *8*, 267.

[104] A. Kumar, H. Biebuyck, N. L. Abbott, G. M. Whitesides, *J. Am. Chem. Soc.* **1992**, *114*, 9188 – 9189.

[105] A. Voet, *Ink and Paper in the Printing Process*, Interscience, New York, **1952**.

[106] P. O. Hidber, W. Helbig, E. Kim, G. M. Whitesides, *Langmuir* **1996**, *12*, 1375 – 1380.

[107] See, for example, a) M. C. Hutley, *Diffraction Gratings*, Academic Press, New York, **1982**; b) B. L. Ramos, S. J. Choquette, *Anal. Chem.* **1996**, *68*, 1245 – 1249.

[108] M. Nakano, N. Nishida, *Appl. Opt.* **1979**, *18*, 3073 – 3074.

[109] D. A. Kiewit, *Rev. Sci. Instrum.* **1973**, *44*, 1741 – 1742.

[110] Replication of features with dimensions below the micron scale has also been used in microscopy to aid in visualizing fragile structures: *Electron Microscopy Preparation Technology Accessories and Consumable*, Bal-TEC Products, Middlebury, CT, **1992**, catalogue no. 5B.

[111] S. L. Goodman, P. A. Sims, R. M. Albrecht, *Biomaterials* **1996**, *17*, 2087 – 2095.

[112] a) F. L. Dickert, S. Thierer, *Adv. Mater.* **1996**, *8*, 987 – 990; b) L. Schweitz, L. I. Anderson, S. Nilsson, *Anal. Chem.* **1997**, *69*, 1179 – 1183; c) D. Kriz, O. Ramström, K. Mosbach, *ibid*. **1997**, *69*, 345A – 349A; d) C. Pinel, P. Loisil, P. Gallezot, *Adv. Mater.* **1997**, *9*, 582 – 585.

[113] a) *Siloxane Polymers* (Eds.: S. J. Clarson, J. A. Semlyen), Prentice-Hall, Engleword, NJ, **1993**; b) J. F. Künzler, *Trends Polym. Sci.* **1996**, *4*, 52 – 59.

[114] Y. Xia, N. Venkateswaran, D. Qin, J. Tien, G. M. Whitesides, *Langmuir* **1998**, *14*, 363 – 371.

[115] A PDMS block that is about 1 mm thick has a transmittance of about 90 % at 325 nm.

[116] Elastomeric mirrors and diffraction gratings: J. L. Wilbur, R. J. Jackman, G. M. Whitesides, E. L. Cheung, L. K. Lee, M. G. Prentiss, *Chem. Mater.* **1996**, *8*, 1380 – 1385.

[117] Elastomeric optical modulators: a) J. A. Rogers, D. Qin, O. J. A. Schueller, G. M. Whitesides, *Rev. Sci. Instrum.* **1996**, *67*, 3310 – 3319; b) J. A. Rogers, O. J. A. Schueller, C. Marzolin, G. M. Whitesides, *Appl. Opt.* **1997**, *36*, 5792 – 5795.

[118] Elastomeric light valves: D. Qin, Y. Xia, G. M. Whitesides, *Adv. Mater.* **1997**, *9*, 407 – 409.

[119] Elastomeric photothermal detectors: J. A. Rogers, R. J. Jackman, O. J. A. Schueller, G. M. Whitesides, *Appl. Opt.* **1996**, *35*, 6641 – 6647.

[120] D. Qin, Y. Xia, A. J. Black, G. M. Whitesides, *J. Vac. Sci. Technol. B* **1998**, in press.

[121] J. A. Rogers, K. E. Paul, R. J. Jackman, G. M. Whitesides, *Appl. Phys. Lett.* **1997**, *70*, 2658 – 2660; *J. Vac. Sci. Technol. B* **1998**, in press.

[122] See, for example, a) G. S. Ferguson, M. K. Chaudhury, G. B. Sigal, G. M. Whitesides, *Science* **1991**, *253*, 776 – 778; b) M. K. Chaudhury, G. M. Whitesides, *ibid*. **1992**, *255*, 1230 – 1232; c) G. S. Ferguson, M. K. Chaudhury, H. A. Biebuyck, G. M. Whitesides, *Macromolecules* **1993**, *26*, 5870 – 5875; d) M. K. Chaudhury, *Biosens. Bioelectron.* **1995**, *10*, 785 – 788.

[123] See, for example, T. Tanaka, M. Morigami, N. Atoda, *Jpn. J. Appl. Phys.* **1993**, *32*, 6059 – 6061.

[124] E. Delamarche, H. Schmid, H. A. Biebuyck, B. Michel, *Adv. Mater.* **1977**, *9*, 741 – 746.

[125] For technical reports on thermally curable PDMS resins, see, for example, Dow Corning, Midland, MI, **1986**.
[126] L. C. DeBolt, J. E. Mark, *Macromolecules* **1987**, *20*, 2369 – 2374.
[127] J. A. Rogers, K. Paul, G. M. Whitesides, *J. Vac. Sci. Technol. B* **1998**, in press.
[128] Y. Xia, A. Zhuk, G. M. Whitesides, unpublished results.
[129] Y. Xia, J. Tien, D. Qin, G. M. Whitesides, *Langmuir* **1996**, *12*, 4033 – 4038.
[130] D. Qin, Y. Xia, G. M. Whitesides, *Adv. Mater.* **1996**, *8*, 917 – 919.
[131] For the economical production of masks using a desk-top publishing system, see M. Parameswaren, http://www.fas.sfu.ca/ensc/research/groups/micromachining/file2.html.
[132] H. A. Biebuyck, G. M. Whitesides, *Langmuir* **1994**, *10*, 4581 – 4587.
[133] N. B. Larsen, H. Biebuyck, E. Delamarche, B. Michel, *J. Am. Chem. Soc.* **1997**, *119*, 3017 – 3026.
[134] See, for example, a) G. P. López, H. A. Biebuyck, G. M. Whitesides, *Langmuir* **1993**, *9*, 1513 – 1516; b) G. B. López, H. A. Biebuyck, R. Härter, G. M. Whitesides, *J. Am. Chem. Soc.* **1993**, *115*, 10774 – 10781.
[135] See, for example, a) C. D. Frisbie, L. F. Rozsnyai, A. Noy, M. S. Wrighton, O. M. Lieber, *Science* **1994**, *263*, 2071 – 2073; b) J. L. Wilbur, H. A. Biebuyck, J. C. MacDonald, G. M. Whitesides, *Langmuir* **1995**, *11*, 825 – 831; c) G. Bar, S. Rubin, A. N. Parikh, B. I. Swanson, T. A. Zawodzinski, Jr., M.-H. Whangbo, *ibid.* **1997**, *13*, 373 – 377.
[136] G. P. López, H. A. Biebuyck, C. D. Frisbie, G. M. Whitesides, *Science* **1993**, *260*, 647 – 649.
[137] J. Heinze, *Angew. Chem.* **1993**, *105*, 1327 – 1349; *Angew. Chem. Int. Ed. Engl.* **1993**, *32*, 1268 – 1288.
[138] J. C. C. Tsai in *VLSI Technology* (Ed.: S. M. Sze), McGraw-Hill, New York, **1988**, pp. 272 – 326.
[139] C. Kittel, *Introduction to Solid State Physics*, 6th ed., Wiley, New York, **1986**, p. 110.
[140] a) N. L. Jeon, K. Finnie, K. Branshaw, R. G. Nuzzo, *Langmuir* **1997**, *13*, 3382 – 3391; b) A. N. Parikh, M. A. Schivley, E. Koo, K. Seshadri, D. Aurentz, K. Mueller, D. L. Allara, *J. Am. Chem. Soc.* **1997**, *119*, 3135 – 3143.
[141] Y. Xia, X.-M. Zhao, E. Kim, G. M. Whitesides, *Chem. Mater.* **1995**, *7*, 2332 – 2337.
[142] Selective wetting and dewetting: a) A. Kumar, G. M. Whitesides, *Science* **1994**, *263*, 60 – 62; b) H. A. Biebuyck, G. M. Whitesides, *Langmuir* **1994**, 10, 2790 – 2793; c) S. Palacin, P. C. Hidber, J.-P. Bourgoin, C. Miramond, C. Fermon, G. M. Whitesides, *Chem. Mater.* **1996**, *8*, 1316 – 1325; d) C. B. Gorman, H. A. Biebuyck, G. M. Whitesides, *ibid*. **1995**, *7*, 252 – 254; e) E. Kim, G. M. Whitesides, *ibid*. **1995**, *7*, 1257 – 1264; f) E. Kim, G. M. Whitesides, L. K. Lee, S. P. Smith, M. Prentiss, *Adv. Mater.* **1996**, *8*, 139 – 142.
[143] Selective attachment of cells: a) R. Singhvi, A. Kumar, G. P. Lopez, G. P. Stephanopoulos, D. I. C. Wang, G. M. Whitesides, D. E. Ingber, *Science* **1994**, *264*, 696 – 698; b) M. Mrksich, C. S. Chen, Y. Xia, L. E. Dike, D. E. Ingber, G. M. Whitesides, *Proc. Natl. Acad. Sci. USA* **1996**, *93*, 10775 – 10778; c) C. S. Chen, M. Mrksich, S. Huang, G. M. Whitesides, D. E. Ingber, *Science* **1997**, *276*, 1245 – 1248; d) M. Mrksich, L. E. Dike, J. Tien, D. E. Ingber, G. M. Whitesides, *Exp. Cell Res.* **1997**, *235*, 305 – 313.
[144] Selective deposition of polymers: a) C. B. Gorman, H. A. Biebuyck, G. M. Whitesides, *Chem. Mater.* **1995**, *7*, 526 – 529; b) P. Hammond, G. M. Whitesides, *Macromolecules* **1995**, *28*, 7569 – 7571; c) C. N. Sayre, D. M. Collard, *Langmuir* **1997**, *13*, 714 – 722; d) *J. Mater. Chem.* **1997**, *7*, 909 – 912; e) Z. Huang, P.-C. Wang, A. G. MacDiarmid, Y. Xia, G. M. Whitesides, *Langmuir* **1997**, *13*, 6480 – 6484.
[145] Selective CVD of copper and dielectric oxides: a) N. L. Jeon, R. G. Nuzzo, Y. Xia, M. Mrksich, G. M. Whitesides, *Langmuir* **1995**, *11*, 3024 – 3026; b) N. L. Jeon, P. G. Clem, R. G. Nuzzo, D. A. Payne, *J. Mater. Res.* **1995**, *10*, 2996 – 2999; c) N. L. Jeon, P. G. Clem, D. A. Payne, R. G. Nuzzo, *Langmuir* **1996**, *12*, 5350 – 5355; d) H. Yang, N. Coombs, G. A. Ozin, *Adv. Mater.* **1997**, *9*, 811 – 814.
[146] V. K. Gupta, N. L. Abbott, *Science* **1997**, *276*, 1533 – 1536.
[147] Y. Xia, D. Qin, G. M. Whitesides, *Adv. Mater.* **1996**, *8*, 1015 – 1017.
[148] a) Y. Xia, G. M. Whitesides, *J. Am. Chem. Soc.* **1995**, *117*, 3274 – 3275; b) Y. Xia, G. M. Whitesides, *Adv. Mater.* **1995**, *7*, 471 – 473; C) J. L. Wilbur, E. Kim, Y. Xia, G. M. Whitesides, *ibid*. **1995**, *7*, 649 – 652; d) Y. Xia, G. M. Whitesides, *Langmuir* **1997**, *13*, 2059 – 2067.
[149] R. J. Jackman, J. L.Wilbur, G. M. Whitesides, *Science* **1995**, *269*, 664 – 666.
[150] S. J. Moss in *The Chemistry of the Semiconductor Industry* (Eds.: S. J. Moss, A. Ledwidth), Chapman and Hall, New York, **1987**, pp. 390 – 413.
[151] W. Kern, C. A. Deckert in *Thin Film Processes* (Eds.: J. L. Vossen, E. Kern), Academic Press, New York, **1978**.
[152] a) E. Kim, A. Kumar, G. M. Whitesides, *J. Electrochem. Soc.* **1995**, *142*, 628 – 633; b) E. Kim, G. M. Whitesides, M. B. Freiler, M. Levy, J. L. Lin, R. M. Osgood, Jr., *Nanotechnology* **1996**, *7*, 266 – 269; c) T. K. Whidden, D. K. Ferry, M. N. Kozicki, E. Kim, A. Kumar, J. L. Wilbur, G. M. Whitesides, *ibid*. **1996**, *7*, 447 – 451.
[153] Y. Xia, G. M. Whitesides, *Adv. Mater.* **1996**, *8*, 765 – 768.
[154] K. E. Petersen, *Proc. IEEE* **1982**, *70*, 420 – 457.
[155] Y. Xia, X.-M. Zhao, G. M. Whitesides, unpublished results.
[156] A. Wang, J. Zhao, M. A. Green, *Appl. Phys. Lett.* **1990**, *57*, 602 – 604.
[157] N. Rajkumar, J. N. McMullin, *Appl. Opt.* **1995**, *34*, 2556 – 2559.
[158] A. E. Kaloyeros, M. A. Fury, *MRS Bull.* **1993**, *28*(6), 22 – 28.
[159] J. Li, T. E. Seidel, J. W. Mayer, *MRS Bull.* **1994**, *29*(8), 15 – 18.
[160] R. J. Jackman, J. A. Rogers, G. M. Whitesides, *IEEE Trans. Magn.* **1997**, *33*, 2501 – 2503.
[161] J. A. Rogers, R. J. Jackman, G. M. Whitesides, *J. Microelec. Sys.* **1997**, *6*, 184 – 192.
[162] J. A. Rogers, R. J. Jackman, G. M. Whitesides, J. L. Wagener, A. M. Vengsarkar, *Appl. Phys. Lett.* **1997**, *70*, 7 – 9.
[163] J. A. Rogers, R. J. Jackman, G. M. Whitesides, D. L. Olson, J. V. Sweedler, *Appl. Phys. Lett.* **1997**, *70*, 2464 – 2466.
[164] J. A. Rogers, R. J. Jackman, G. M. Whitesides, *Adv. Mater.* **1997**, *9*, 475 – 477.
[165] a) Y. Xia, G. M. Whitesides, unpublished results; b) C. Marzolin, A. Terfort, J. Tien, G. M. Whitesides, *Thin Solid Films* **1998**, in press.
[166] P. C. Hidber, P. F. Nealey, W. Helbig, G. M. Whitesides, *Langmuir* **1996**, *12*, 5209 – 5215.
[167] Reviews on acid-sensitive photoresists: a) E. Reichmanis, F. M. Houlihan, O. Nalamasu, T. X. Neenan, *Adv. Mater. Opt. Electron.* **1994**, *4*, 83 – 93; b) S. A. MacDonald, C. Willson, J. M. J. Frechet, *Acc. Chem. Res.* **1994**, *27*, 151 – 158.
[168] G. M. Whitesides, Y. Xia, *Photonics Spectra* **1997**, *31*(1), 90 – 91.
[169] Y. Xia, J. J. McClelland, R. Gupta, D. Qin, X.-M. Zho, L. L. Sohn, R. J. Celotta, G. M. Whitesides, *Adv. Mater.* **1997**, *9*, 147 – 149.
[170] J. J. McClelland, R. E. Scholten, E. C. Palm, R. J. Celotta, *Science* **1993**, *262*, 877 – 879.
[171] "Technical reports on UV-curable adhesives": Norland Products Inc., New Brunswick, NJ, USA.
[172] A. Suzuki, K. Tada, *Thin Solid Films* **1980**, *72*, 419 – 426.
[173] L. R. Dalton, A. W. Harper, B. Wu, R. Ghosn, J. Laquindanum, Z. Liang, A. Hubbel, C. Xu, *Adv. Mater.* **1995**, *7*, 519 – 540.
[174] See, for example, a) E. Ozbay, E. Michel, G. Tuttle, R. Biswas, M. Sigalas, K. M. Ho, *Appl. Phys. Lett.* **1994**, *64*, 2059 – 2061; b) J. D. Joannopoulos, P. R. Villeneuve, S. Fan, *Nature* **1997**, *386*, 143 – 149.
[175] N. A. Peppas, R. Langer, *Science* **1994**, *263*, 1715 – 1720.
[176] X.-M. Zhao, S. P. Smith, S. J. Waldman, G. M. Whitesides, M. Prentiss, *Appl. Phys. Lett.* **1997**, *71*, 1017 – 1019.
[177] a) O. J. A. Schueller, S. T. Brittain, G. M. Whitesides, *Adv. Mater.* **1997**, *9*, 477 – 480; b) O. J. A. Schueller, S. T. Brittain, C. Marzolin, G. M. Whitesides, *Chem. Mater.* **1997**, *9*, 1399 – 1406.
[178] C. Marzolin, S. P. Smith, M. Prentiss, G. M. Whitesides, *Adv. Mater.* **1997**, submitted.
[179] Y. Xia, E. Kim, G. M. Whitesides, *Chem. Mater.* **1996**, *8*, 1558 – 1567.
[180] Y. Xia, G. M. Whitesides, unpublished results.
[181] X.-M. Zhao, A. Stoddart, S. P. Smith, E. Kim, Y. Xia, M. Prentiss, G. M. Whitesides, *Adv. Mater.* **1996**, *8*, 420 – 424.
[182] Y. Xia, G. M. Whitesides, unpublished results.
[183] E. Kim, Y. Xia, G. M. Whitesides, *Adv. Mater.* **1996**, *8*, 245 – 247.
[184] E. Kim, Y. Xia, G. M. Whitesides, *J. Am. Chem. Soc.* **1996**, *118*, 5722 – 5731.
[185] a) M. Trau, N. Yao, E. Kim, Y. Xia, G. M. Whitesides, I. A. Aksay, *Nature* **1997**, *390*, 674 – 676; b) M. J. Lochhead, P. Yager, *Mater. Res. Soc. Symp. Proc.* **1997**, *444*, 105 – 110.
[186] E. Delamarche, A. Bernard, H. Schmid, B. Michel, H. Biebuyck, *Science* **1997**, *276*, 779 – 781.
[187] Filling of carbon nanotubes: a) P. M. Ajayan, S. Iijima, *Nature* **1993**, *361*, 333 – 334; b) E. Dujardin, T. W. Ebbesen, H. Hiura, K. Tanigaki, *Science* **1994**, *265*, 1850 – 1852.

[188] Filling of nanometer-sized pores in membranes: C. R. Martin, *Science* **1994**, *266*, 1961 – 1966.
[189] E. Kim, G. M. Whitesides, *J. Phys. Chem. B* **1997**, *101*, 855 – 863.
[190] D. Myers, *Surfaces, Interfaces, and Colloids*, VCH, New York, **1991**, pp. 87 – 109.
[l91] a) P. G. de Gennes, *Rev. Mod. Phys.* **1985**, *57*, 827 – 863; b) M. Dong, F. A. Dullien, I. Chatzis, *J. Coll. Interf. Sci.* **1995**, *172*, 21 – 31; c) M. Dong, I. Chatzis, *ibid*. **1995**, *172*, 278 – 288.
[192] See, for example, a) I. Peterson, *Sci. News* **1995**, *148*, 296 – 197; b) J. M. Weissman, H. B. Sunkara, A. S. Tse, S. A. Asher, *Science* **1996**, *274*, 959 – 960.
[193] See, for example, a) F. Gamier, R. Hajlaoui, A. Yassar, F. Srivastava, *Science* **1994**, *265*, 1684 – 1686; b) Z. Bao, Y. Feng, A. Dodabalapur, V. R. Raju, A. J. Lovinger, *Chem. Mater.* **1997**, *9*, 1299 – 1301.
[194] N. L. Jeon, P. G. Clem, D. Y. Jung, W. B. Lin, G. S. Girolami, D. A. Payne, R. G. Nuzzo, *Adv. Mater.* **1997**, *9*, 891 – 895.
[195] J. Hu, T. Deng, G. M. Whitesides, unpublished results.
[196] J. Hu, R. G. Beck, T. Deng, R. M. Westervelt, K. D. Maranowski, A. C. Gossard, G. M. Whitesides, *Appl. Phys. Lett.* **1997**, *71*, 2020 – 2022.
[197] N.-L. Jeon, J. Hu, M. K. Erhardt, R. G. Nuzzo, G. M. Whitesides, unpublished results.